

A closer look at secondary antiproton production in cosmic rays and its impact on dark matter indirect searches

Andrea Vittino (RWTH Aachen University)

In collaboration with Alejandro Ibarra and Franz Zimma (TUM, Munich)

Lorentz.
center

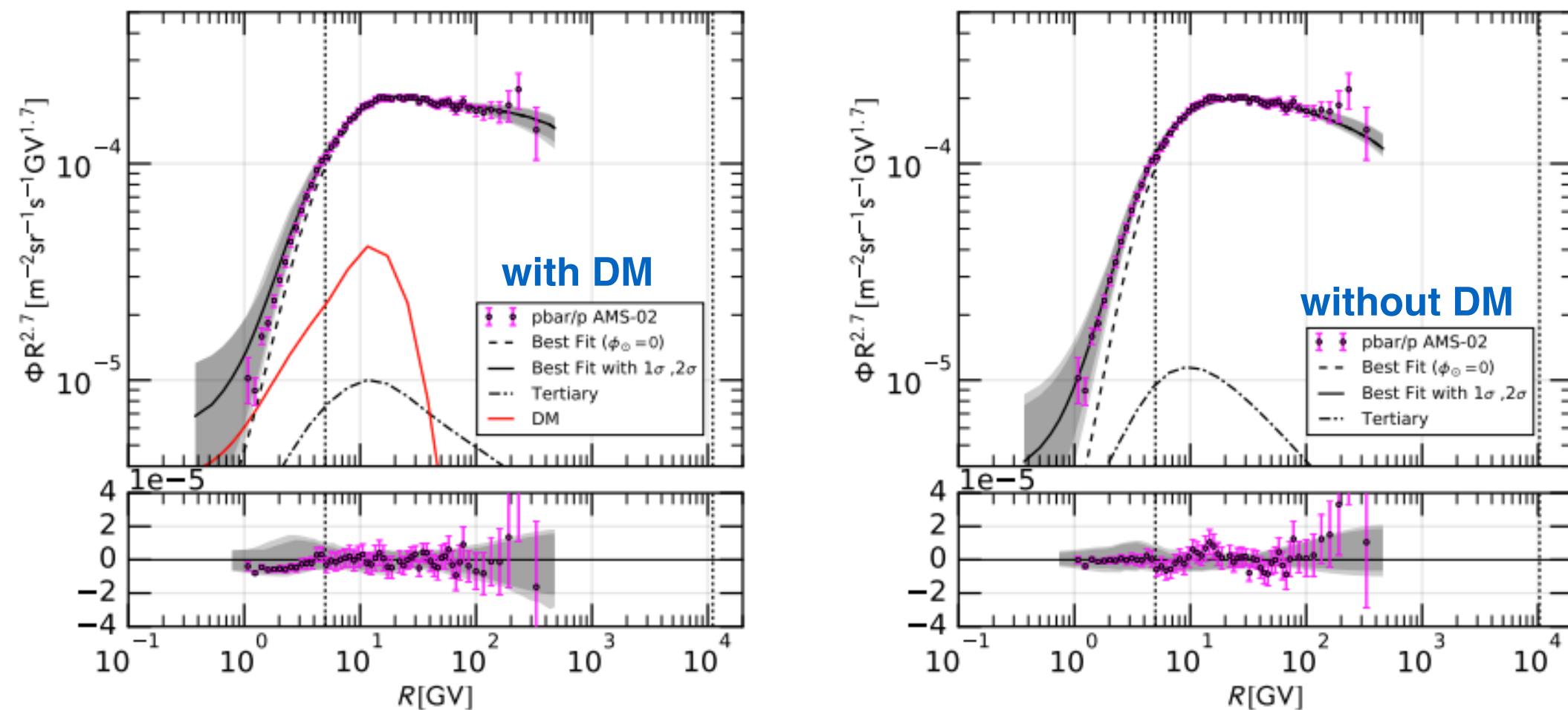
Workshop @Snellius

**Light Anti-Nuclei as a Probe
for New Physics**

14 - 18 October 2019, Leiden, the Netherlands

dark matter searches with CR antiprotons

From **2016**, different studies found an intriguing indication for a **DM signal** in the antiproton flux, for **DM masses near 80 GeV**, with a hadronic annihilation cross-section close to the **thermal value**



Cuoco, Krämer, Korsmeier, Phys.Rev.Lett. 118 (2017)

(analogous results in Cui et al. Phys.Rev.Lett. 118 (2017))

dark matter searches with CR antiprotons

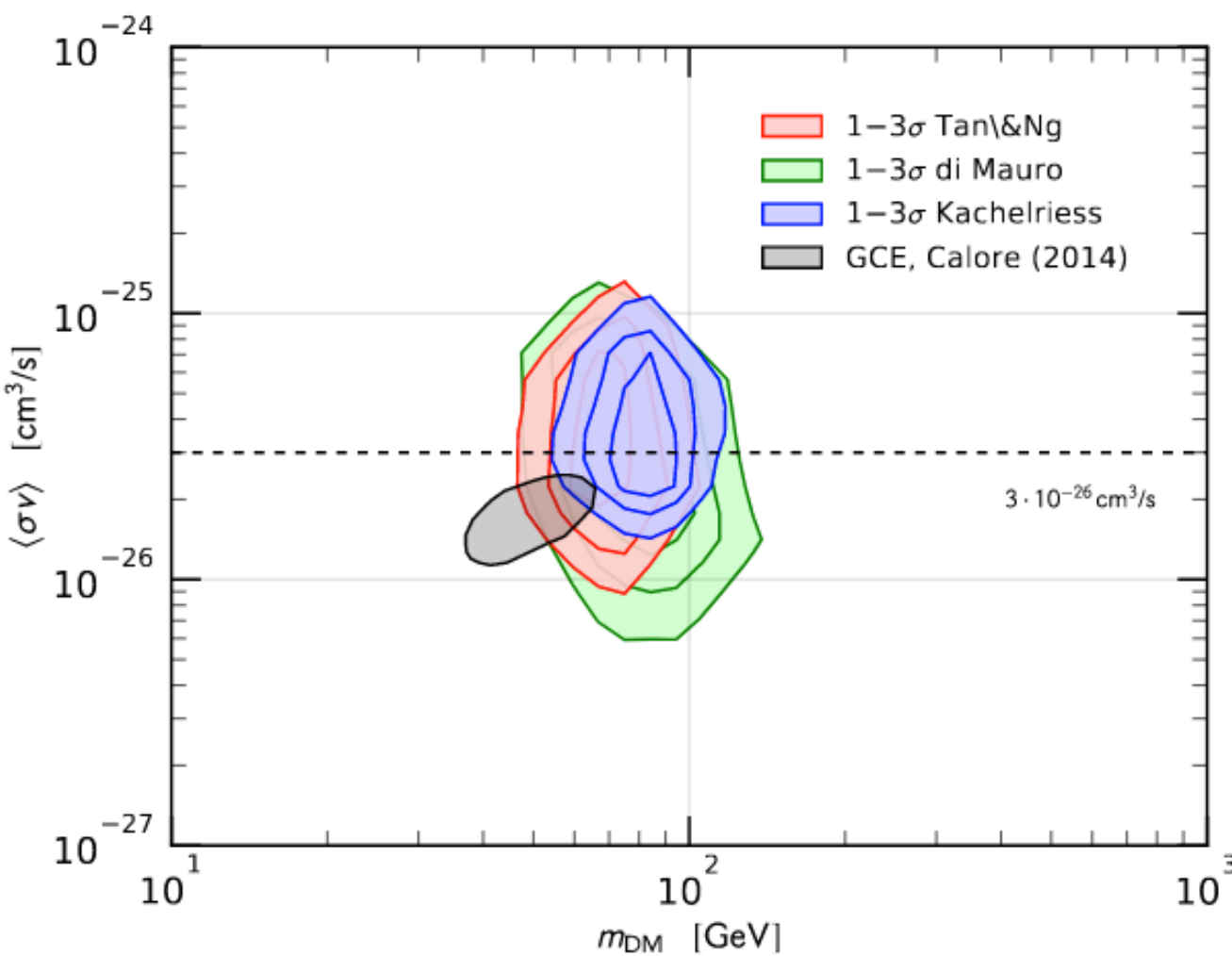


fig. from Cuoco, Krämer, Korsmeier, Phys.Rev.Lett. 118 (2017)

A DM candidate of this kind could potentially **fit** also the **Galactic Centre excess in gamma-rays**.

Recently, several authors have conducted **in-depth investigations** on different aspects of the analysis:

- ▶ Secondary antiproton production cross section
- ▶ Solar modulation
- ▶ Correlation among the data

The **debate is going on**, as some authors claim **the excess is robust**, while others claim that AMS antiprotons are **compatible with a pure secondary origin**.

this talk

We will focus on the **secondary antiproton production cross section**.

In particular, we will consider the **very low-energy regime**, close to the **production threshold**.

First, we will describe **how this cross section is modelled** and we will discuss some **potential shortcomings** of the models that are actually used.

Then, we will describe a **simple analytical model** to study the **effects** that the modelling of this cross section has on the **secondary antiproton spectrum** and on the **bounds on dark matter annihilation cross section**.

secondary antiproton production cross section

We focus here on **data-driven parametrizations**. Alternative : Monte Carlo models

We consider the parametrisation by **Winkler** (from **Kappl and Winkler JCAP 09 (2014)** and **Winkler JCAP 02 (2017)**)

Let's consider a $p + p$ collision. The total cross section is given by the sum of **different channels** :

$$\sigma_{pp \rightarrow \bar{p}} = \sigma_{\bar{p}}^0 + \sigma_{\bar{p}}^\Lambda + \sigma_{\bar{n}}^0$$

direct production Hyperon decay antineutron decay

In terms of the **Lorentz invariant cross section**, we can write:

$$f = E \frac{d^3 \sigma}{dp^3} \quad f_{\bar{p}} = f_{\bar{p}}^0 (2 + \Delta_{IS} + 2\Delta_\Lambda)$$

Δ_{IS} takes into account the **violation of the isospin symmetry**

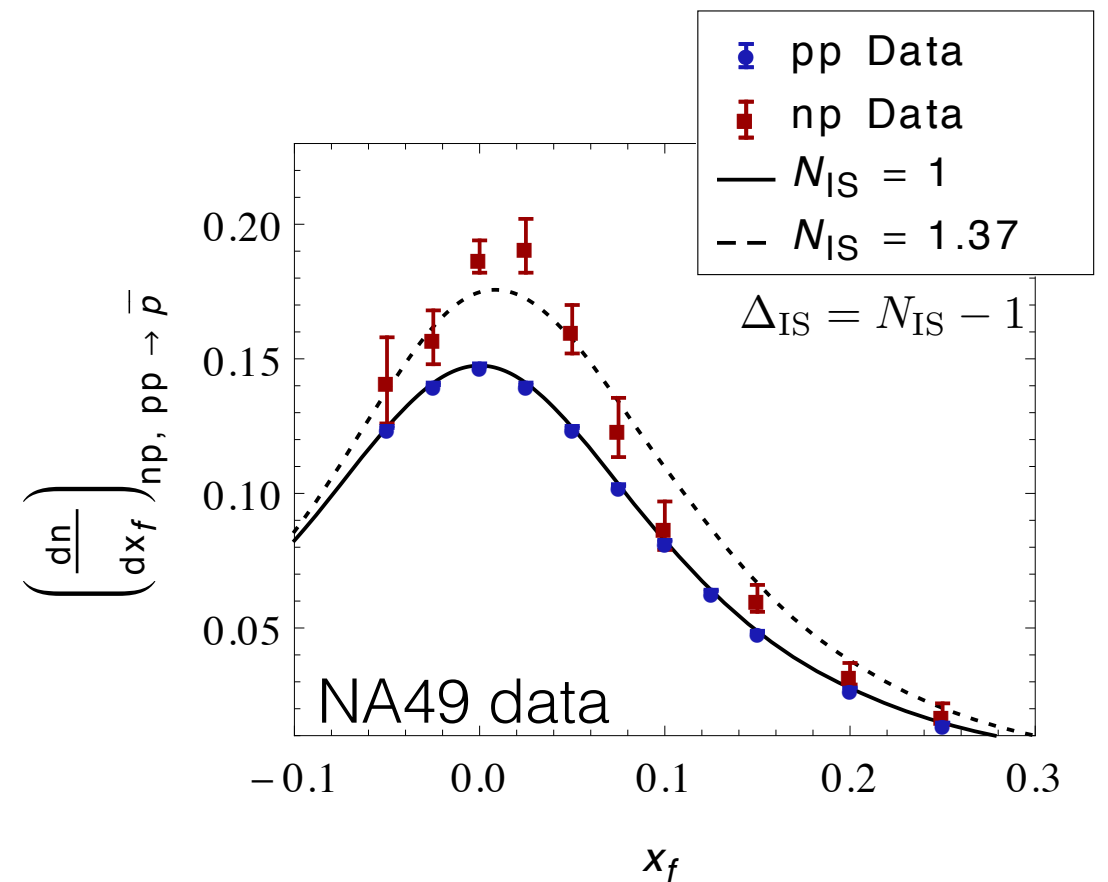


fig. from **Kappl and Winkler JCAP 09 (2014)**

secondary antiproton production cross section

We focus here on **data-driven parametrizations**. Alternative : Monte Carlo models

We consider the parametrisation by **Winkler** (from **Kappl and Winkler JCAP 09 (2014)** and **Winkler JCAP 02 (2017)**)

Let's consider a $p + p$ collision. The total cross section is given by the sum of **different channels** :

$$\sigma_{pp \rightarrow \bar{p}} = \sigma_{\bar{p}}^0 + \sigma_{\bar{p}}^\Lambda + \sigma_{\bar{n}}^0$$

direct production Hyperon decay antineutron decay

In terms of the **Lorentz invariant cross section**, we can write:

$$f = E \frac{d^3 \sigma}{dp^3} \quad f_{\bar{p}} = f_{\bar{p}}^0 (2 + \Delta_{IS} + 2\Delta_\Lambda)$$

Δ_λ is the **ratio** of **hyperon-induced** to **promptly-induced** antiprotons

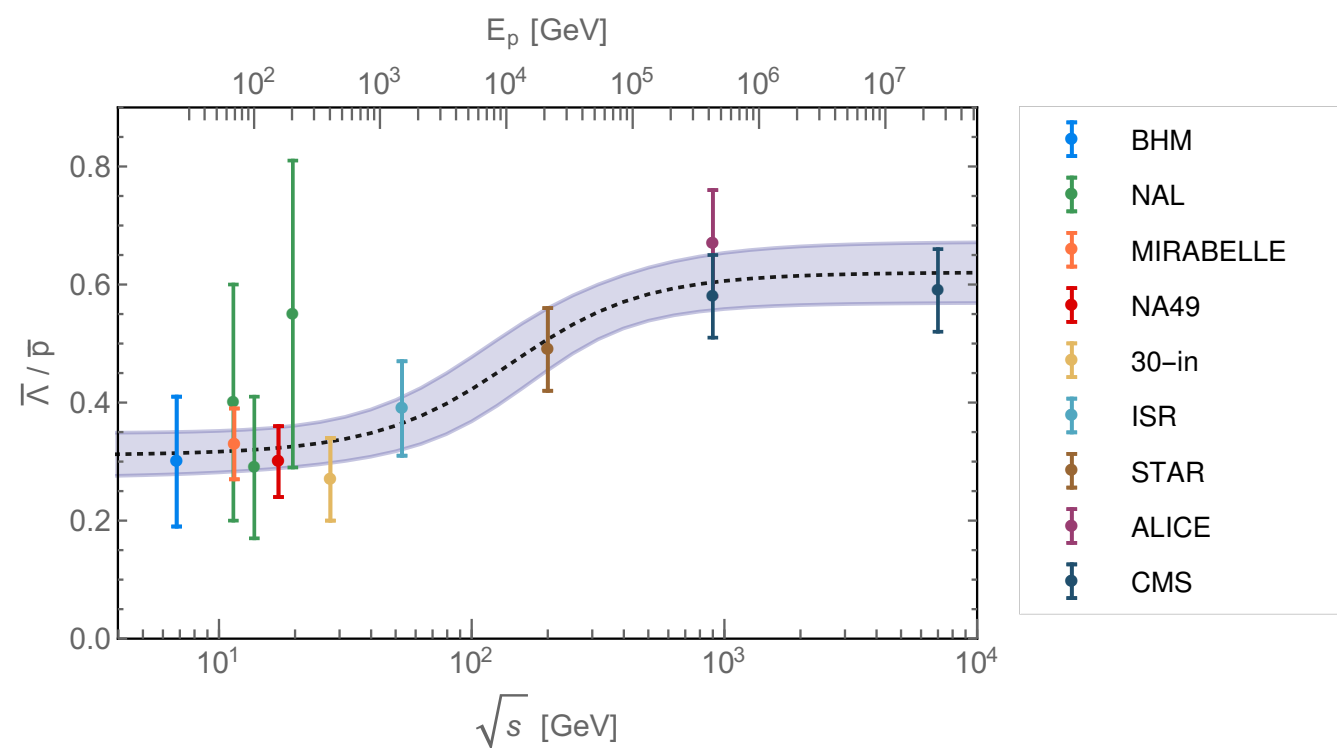


fig. from **Winkler JCAP 02 (2017)**

secondary antiproton production cross section

We focus here on **data-driven parametrizations**. Alternative : Monte Carlo models

We consider the parametrisation by **Winkler** (from **Kappl and Winkler JCAP 09 (2014)** and **Winkler JCAP 02 (2017)**)

We exploit the **radial scaling hypothesis** (which hold at c.m. energies > 10 GeV and not too large), that is:

$$f_{\bar{p}}^0(\sqrt{s}, x_R, p_T) \longrightarrow f_{\bar{p}}^0(x_R, p_T)$$

with $x_R = \frac{E_{\bar{p}}^*}{E_{\bar{p},\max}^*}$

The **fit to the available experimental data** gives:

$$f_{\bar{p}}^0 = 399 \text{ mb} (1 - x_R)^{7.76} \exp\left(-\frac{m_T}{0.168 \text{ GeV}}\right)$$

At **low c.m. energies** (below 10 GeV),

$$f_{\bar{p}}^0 \longrightarrow R f_{\bar{p}}^0$$

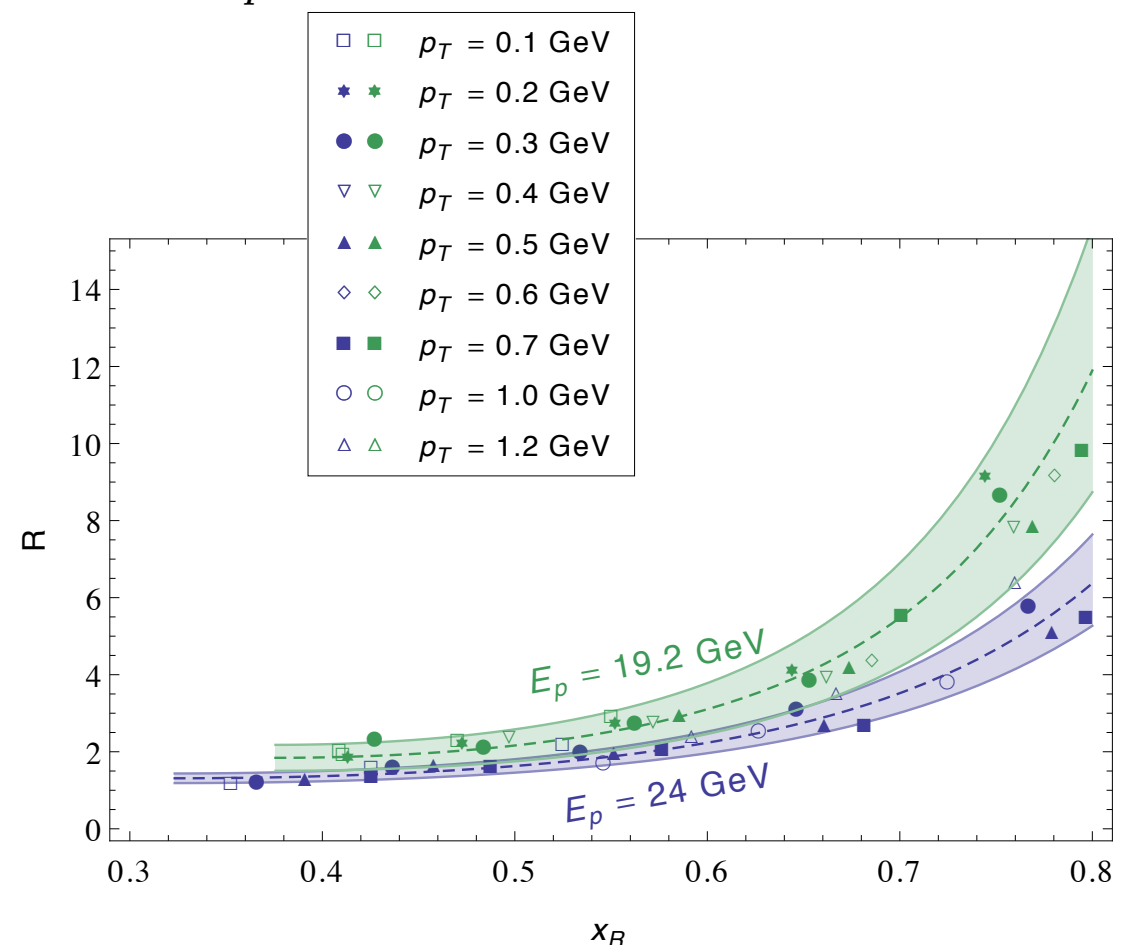
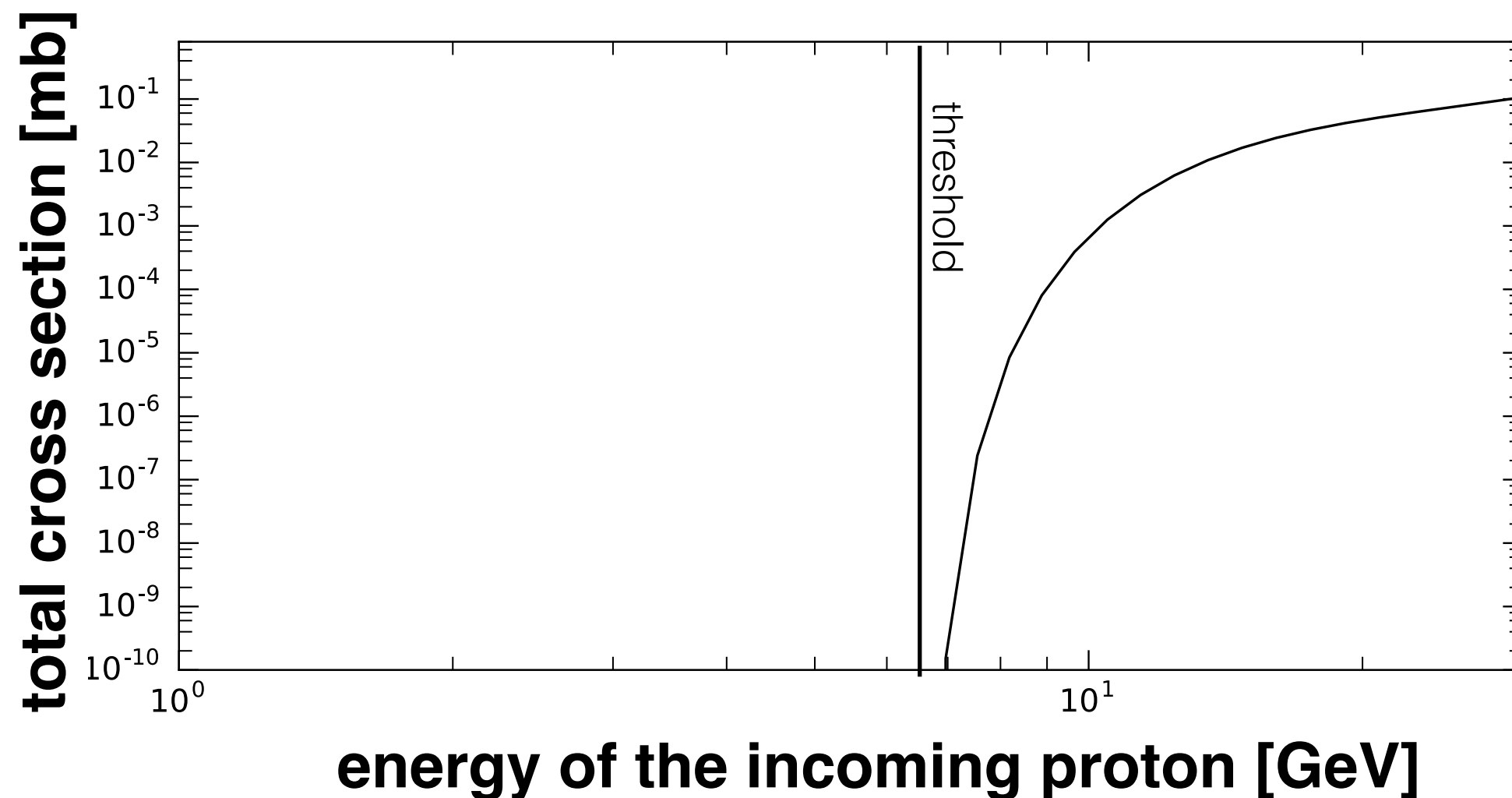


fig. from **Kappl and Winkler JCAP 09 (2014)**

secondary antiproton production cross section

We focus here on **data-driven parametrizations**. Alternative : Monte Carlo models (but, in general, less reliable at low energies, which is the focus here).

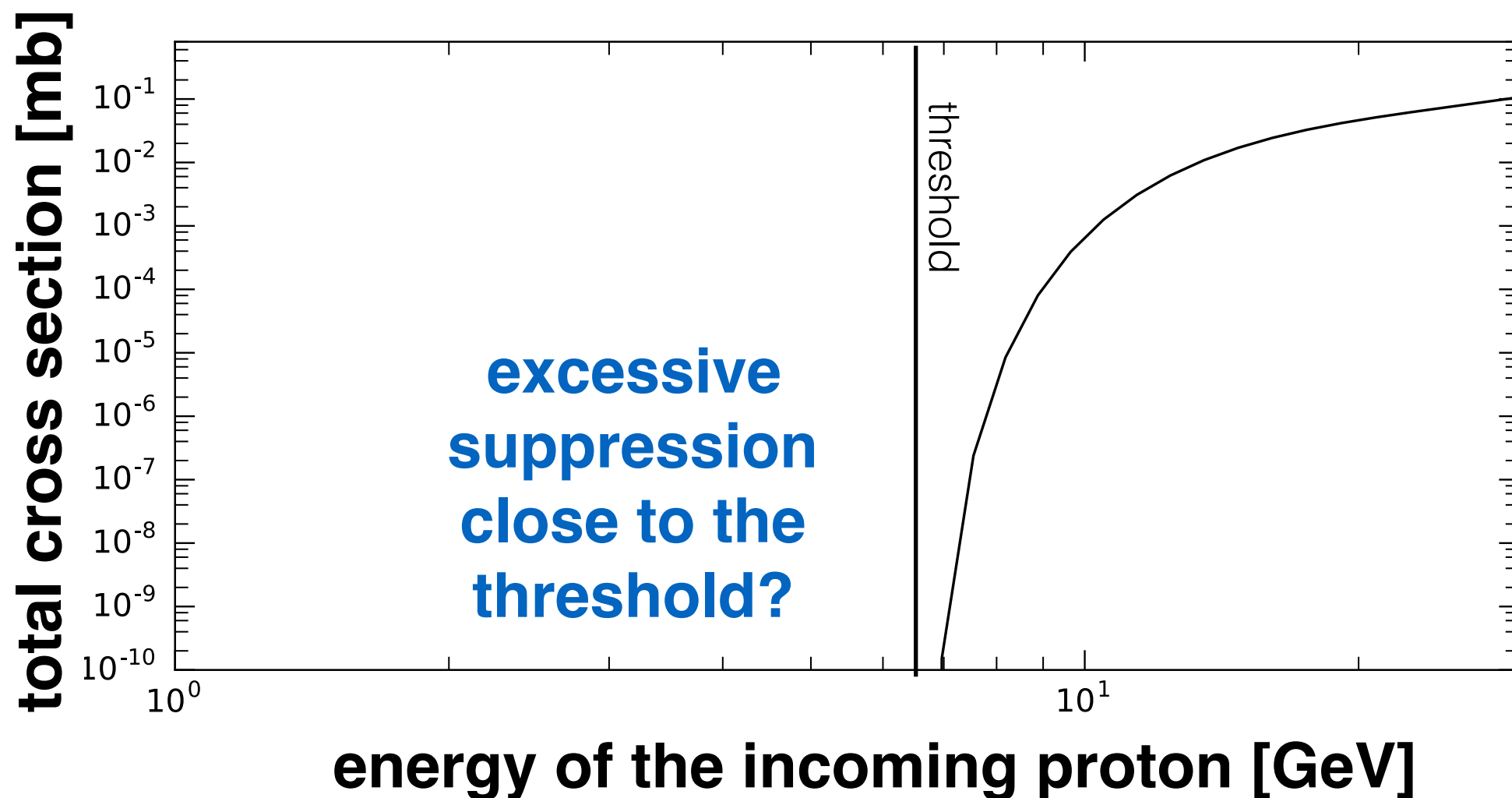
We consider the parametrisation by **Winkler** (from **Kappl and Winkler JCAP 09 (2014)** and **Winkler JCAP 02 (2017)**)



secondary antiproton production cross section

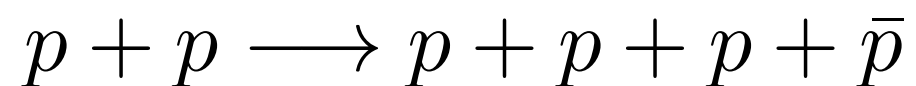
We focus here on **data-driven parametrizations**. Alternative : Monte Carlo models (but, in general, less reliable at low energies, which is the focus here).

We consider the parametrisation by **Winkler** (from **Kappl and Winkler JCAP 09 (2014)** and **Winkler JCAP 02 (2017)**)



low energies - the phase space model

We want to model the **very low-energy behaviour** of the cross section that describes the **production of antiprotons in pp collisions**. In particular, we are interested in the reaction:



In general, the cross section for a $2 \rightarrow n$ process can be written as:

$$d\sigma = \frac{(2\pi)^4 |\mathcal{M}|^2}{4\sqrt{(p_1 \cdot p_2) - m_1^2 m_2^2}} d\Phi_n(p_1, p_2; p_3 \dots p_{n+2})$$

with

$$d\Phi_n(P; p_1, \dots, p_n) = \delta^4(P - \sum_{i=1}^n p_i) \prod_{i=1}^n \frac{d^3 p_i}{(2\pi)^3 2E_i}$$

Phase
space term

phase space model: If we assume that the amplitude $|\mathcal{M}|^2$ is **constant**, the cross section is **simply given by the phase space term**.

low energies - the phase space model

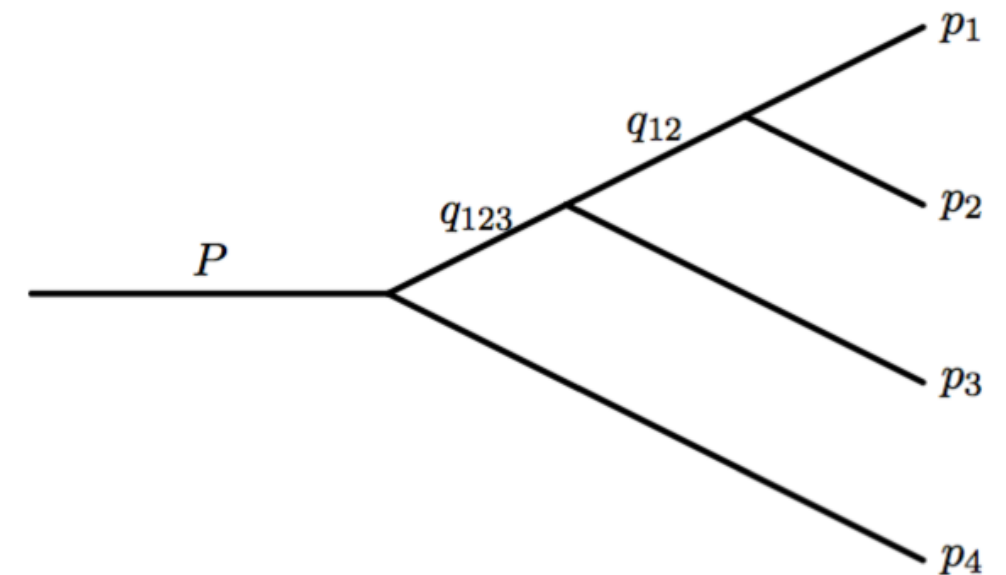
Under the simplifying assumption that the amplitude is constant, the n-body phase space term can be **easily derived in a fully analytical way**

We can decompose the n-body phase space term as follows:

$$\int d\Phi_n(P; p_1, \dots, p_n) = \int \frac{ds_a}{2\pi} \int d\Phi_2(P; q_a, p_n) \int d\Phi_{n-1}(q_a; p_1, \dots, p_{n-1})$$

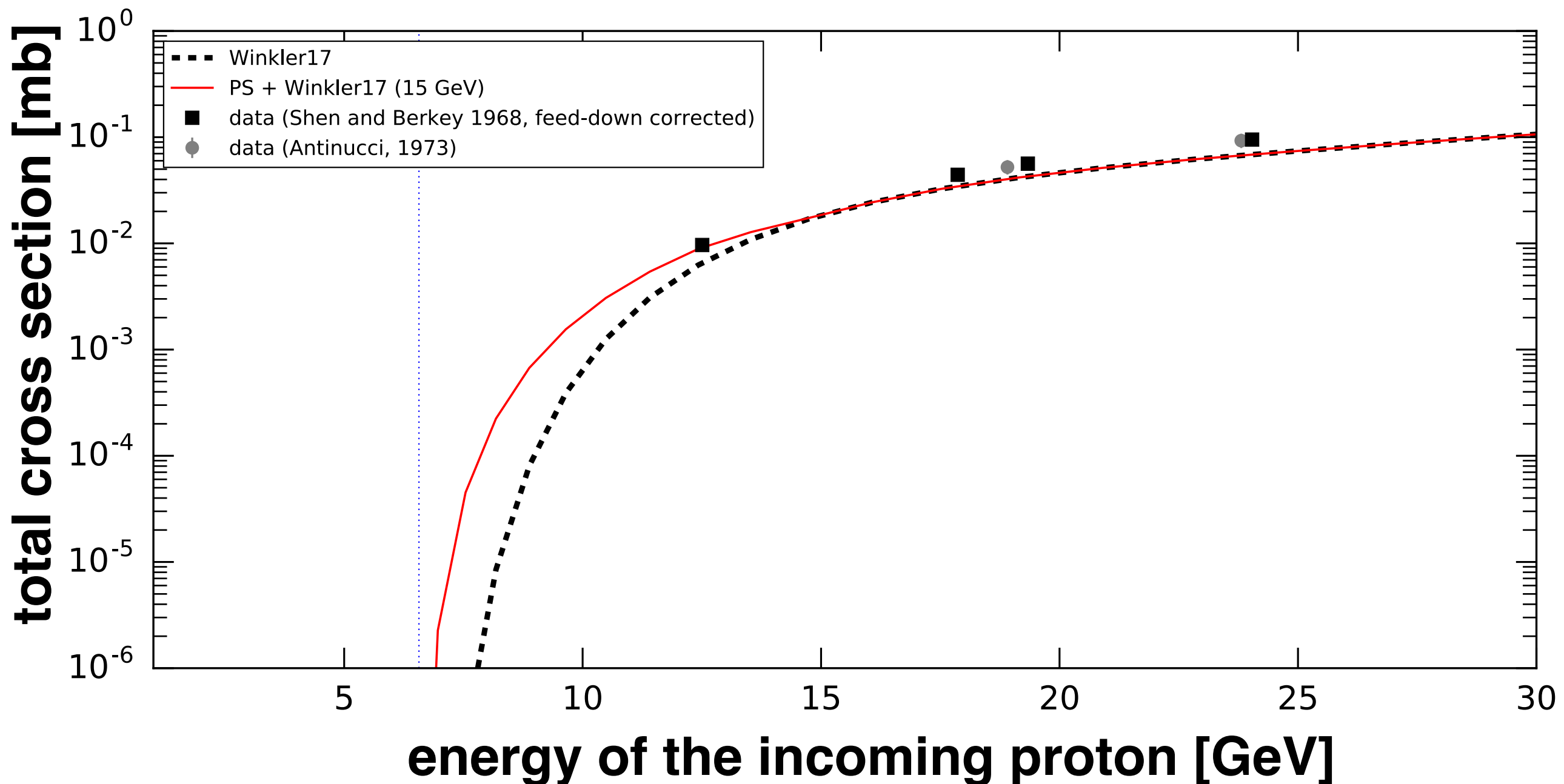
with $a = \{1, \dots, n-1\}$
and the integration limits being:

$$\left(\sum_{i=1}^{n-1} m_i \right)^2 \leq s_a \leq (\sqrt{s} - m_n)^2$$

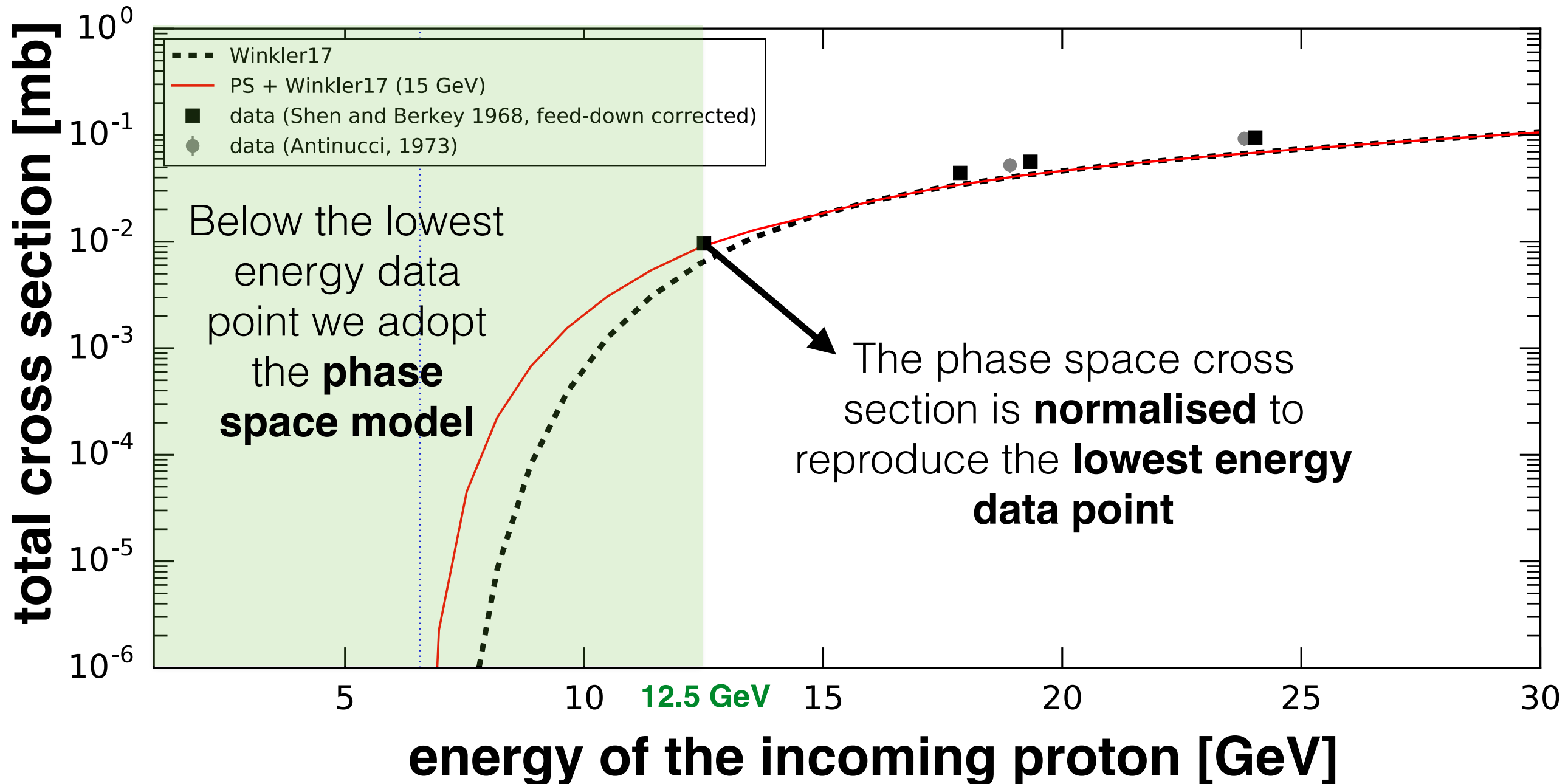


We **iterate** the same procedure until we **only have 2-body phase space terms**, which we can express analytically

our cross section model

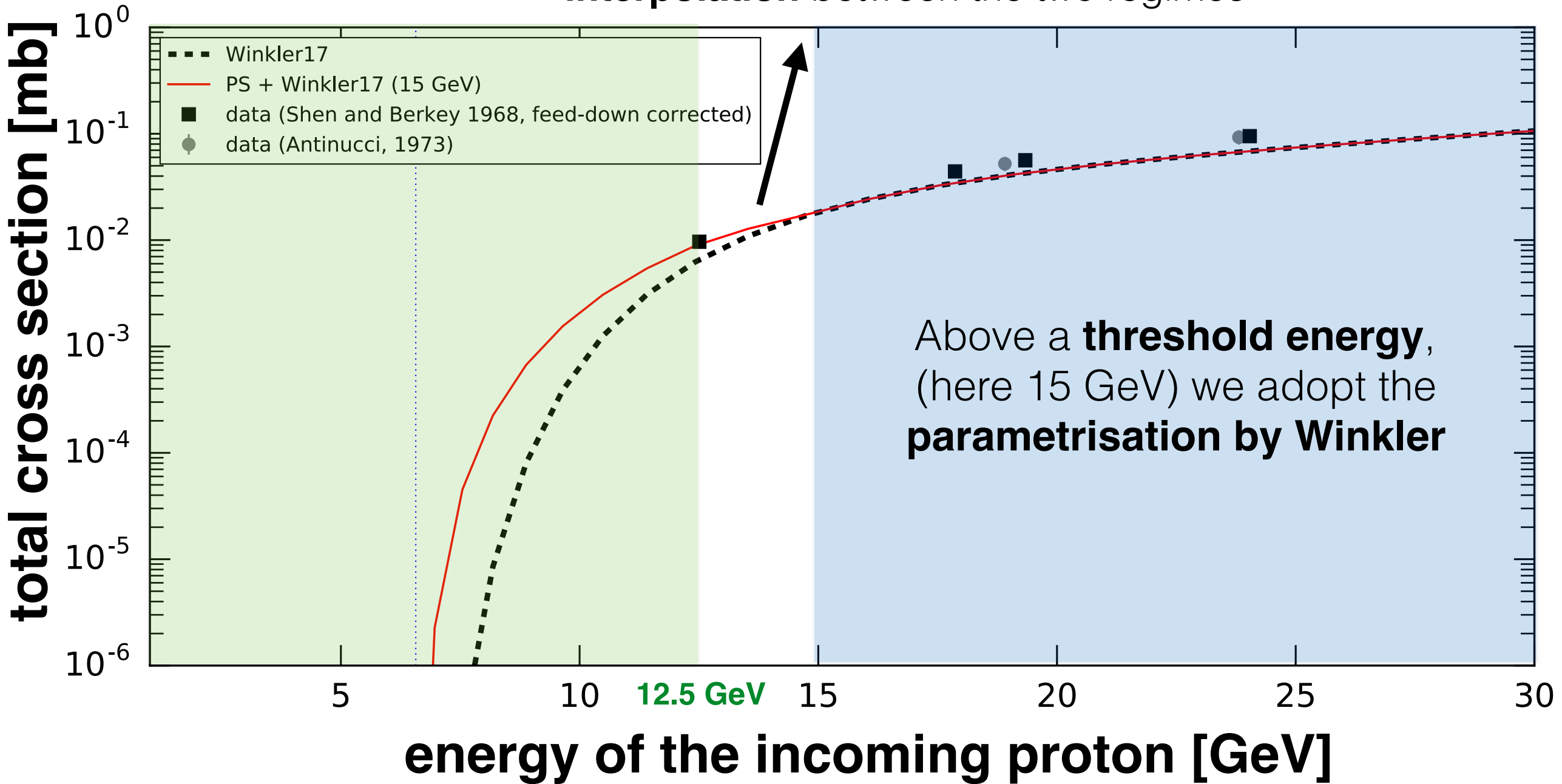


our cross section model



our cross section model

Phase space model, rescaled by means of a **linear interpolation** between the two regimes



The **threshold energy** above which we adopt the Winkler parametrisation
is the only free parameter of our model. How do we constrain it?

comparison with experimental results

- ▶ Data collected in the late '60s at the **CERN PS**.
- ▶ The data consist of the production cross section of antiprotons in **fixed target proton proton collisions**, for energies of the incoming proton of **18.8 GeV and 23.1 GeV** (**Dekkers et al. Phys. Rev. 137, 1965**) and **19.2 GeV** (**Allaby et al. Tech. Rep. CERN 1970**).

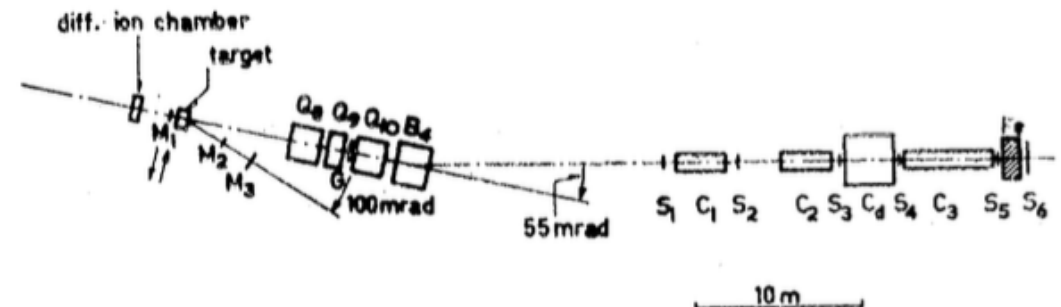


FIG. 1. Experimental layout of the spectrometer and the counter telescope. M_{1-3} , monitor; Q_8-Q_{10} , quadrupole lenses; B_4 , bending magnet; G , guard counters; S_1-S_6 , scintillators; C_1-C_3 , threshold Čerenkov counters; C_d , differential Čerenkov counter; Fe, 1 m iron absorber.

fig. from **Dekkers et al. Phys. Rev. 137 (1965)**

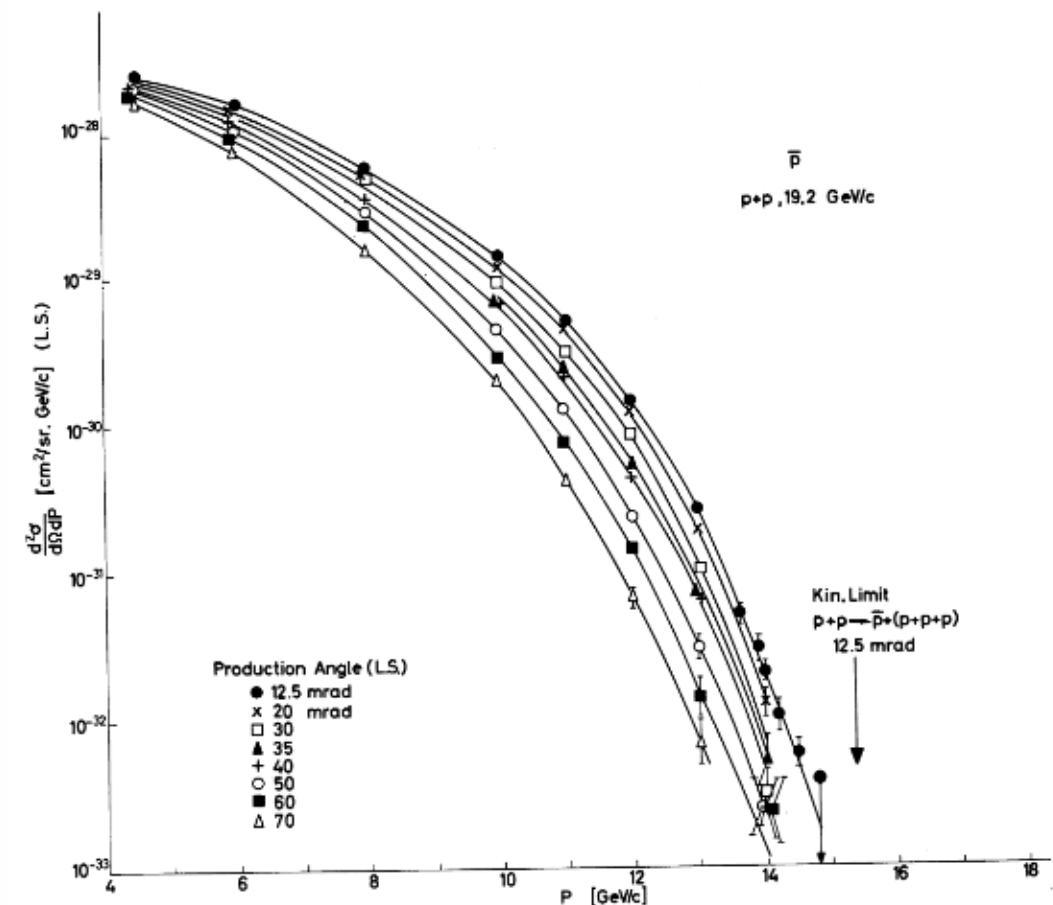
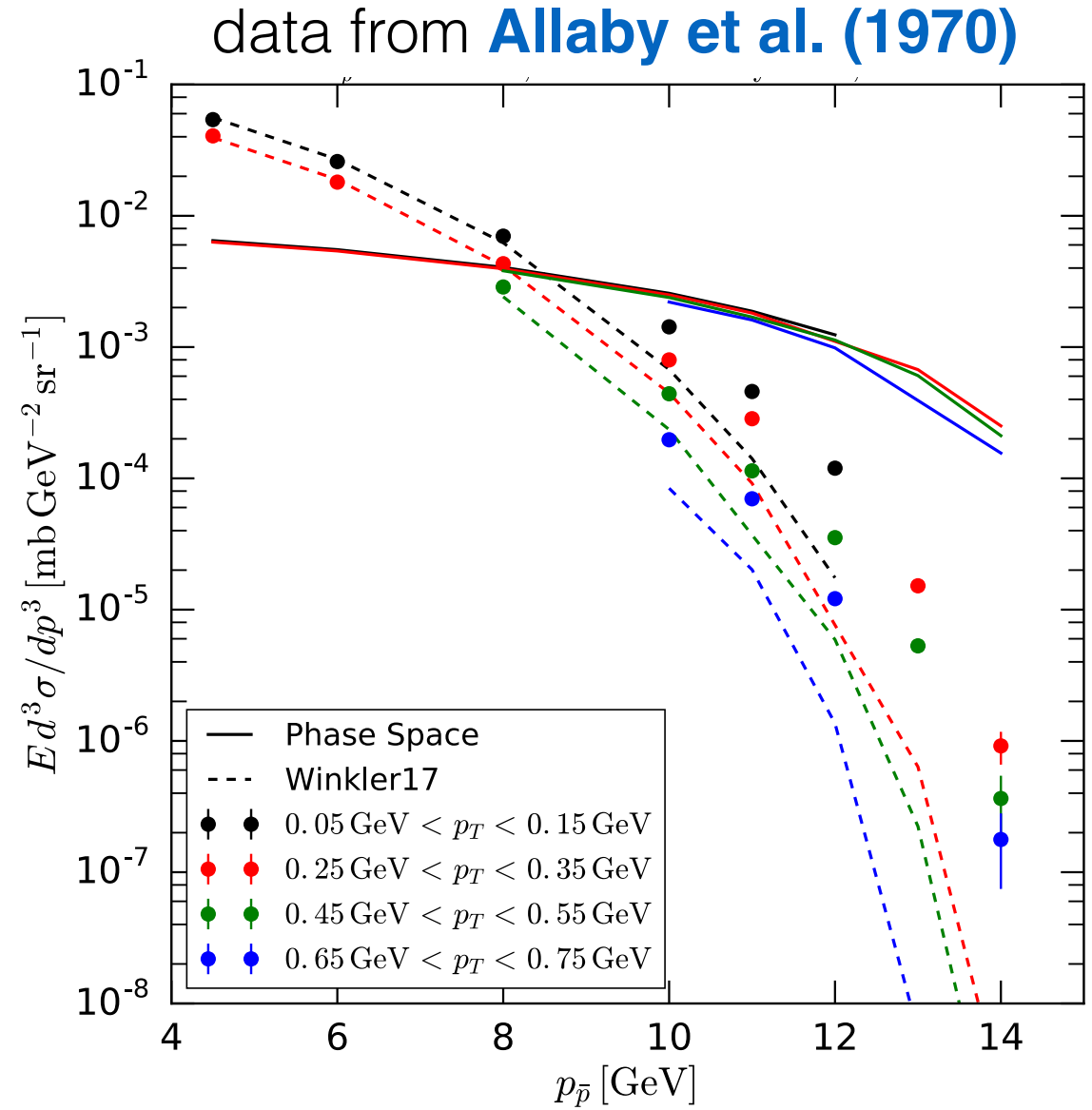
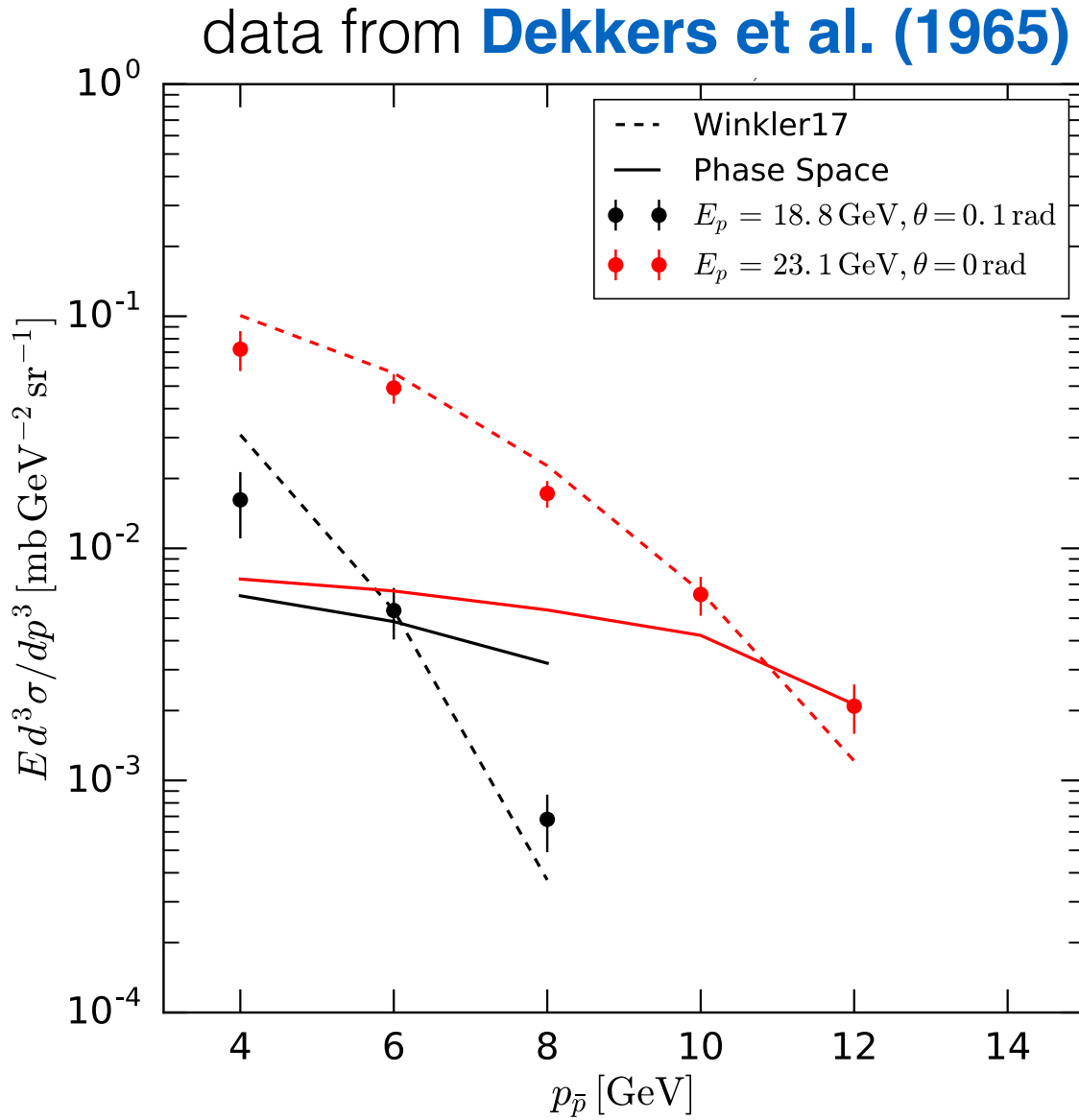


fig. from **Allaby et al. Tech. Rep. CERN (1970)**

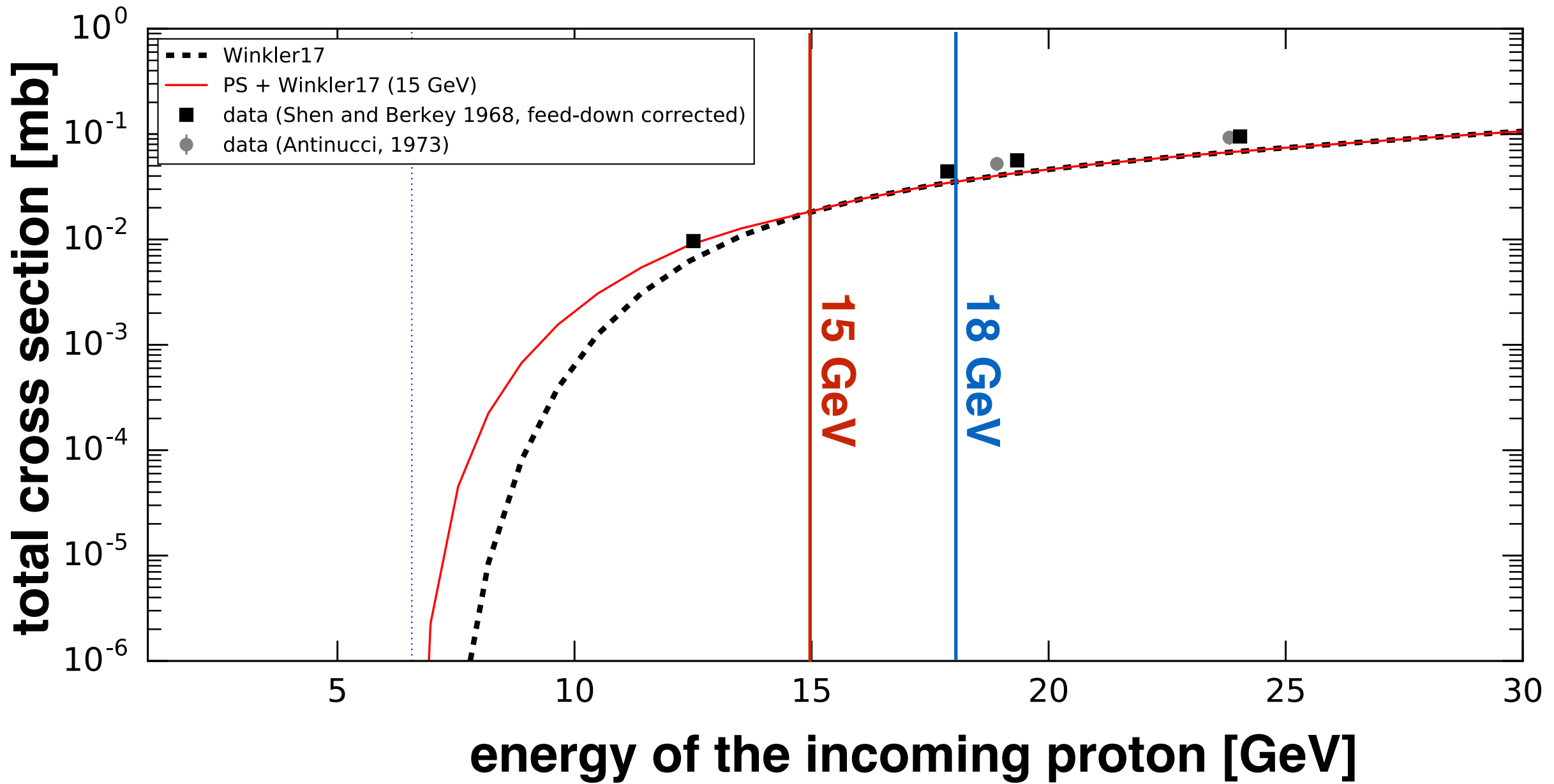
comparison with experimental results



The phase space model **does not seem to provide a good description** of antiproton production at these energies. This gives us an **upper limit to its applicability**.

our cross section model

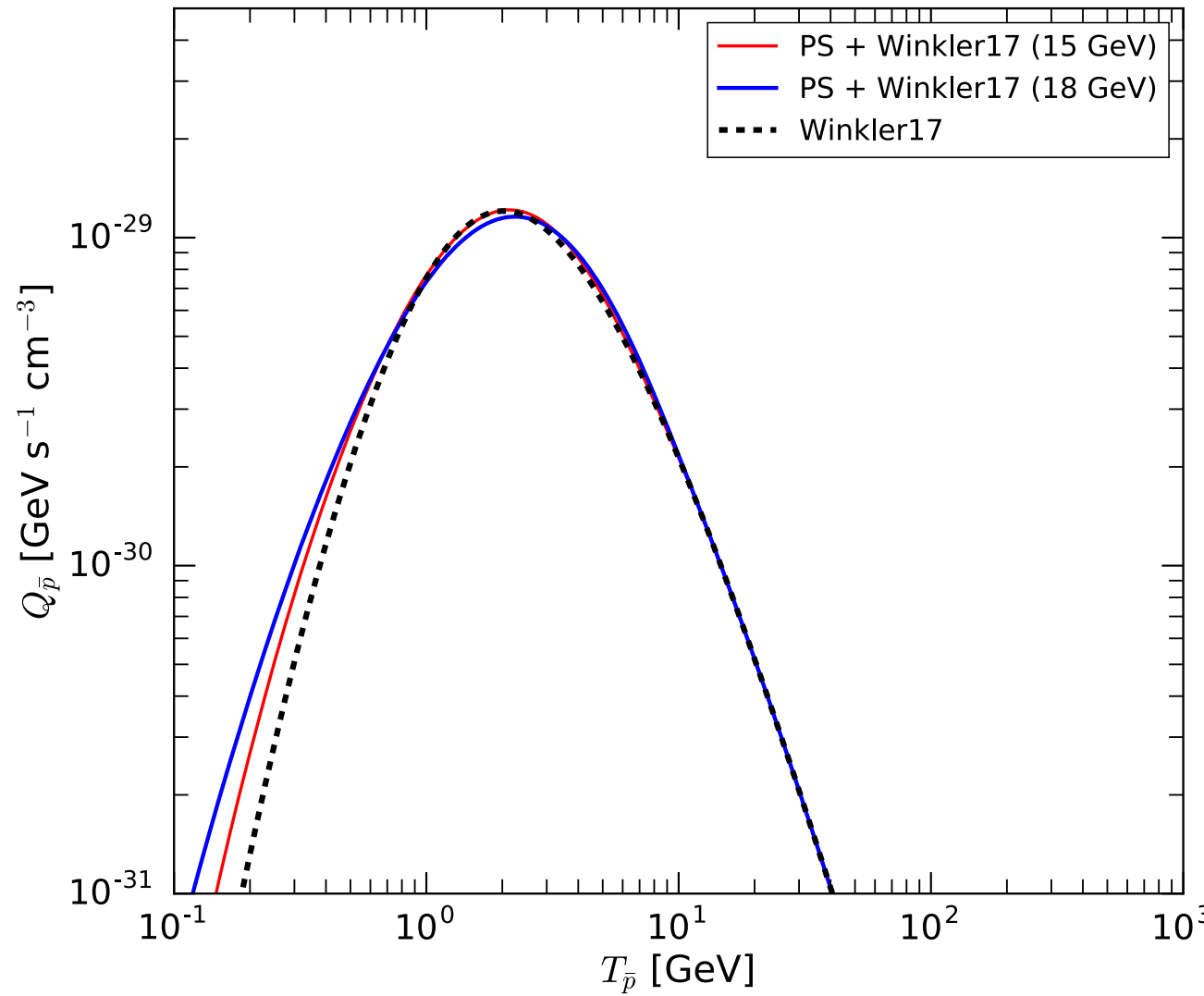
In light of these constraints we consider **two possible values** for the threshold energy: **15 GeV** and **18 GeV**



This is the cross section for the promptly-produced antiprotons. We obtain the total cross section by using Δ_{IS} and Δ_λ as determined by Winkler

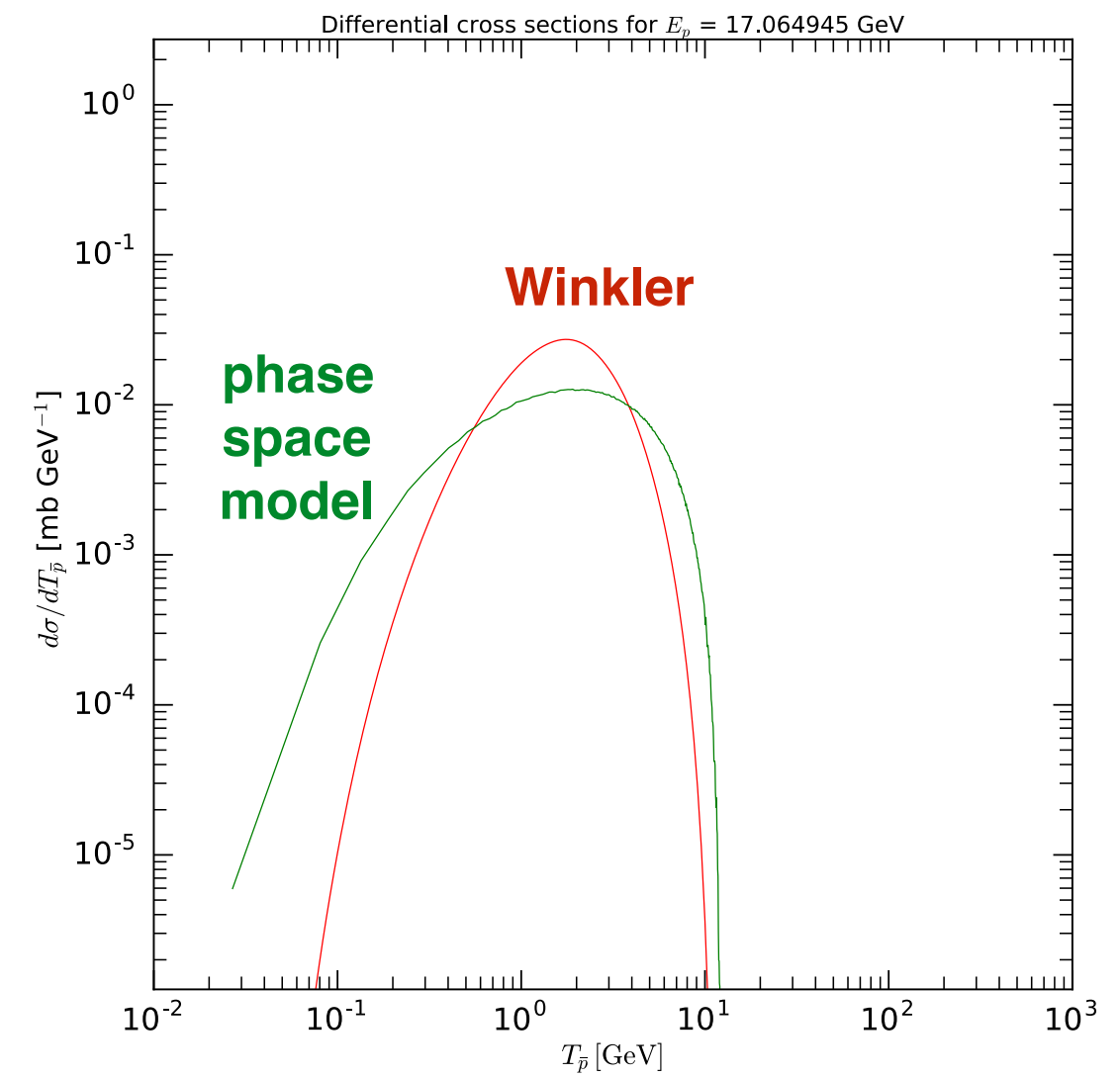
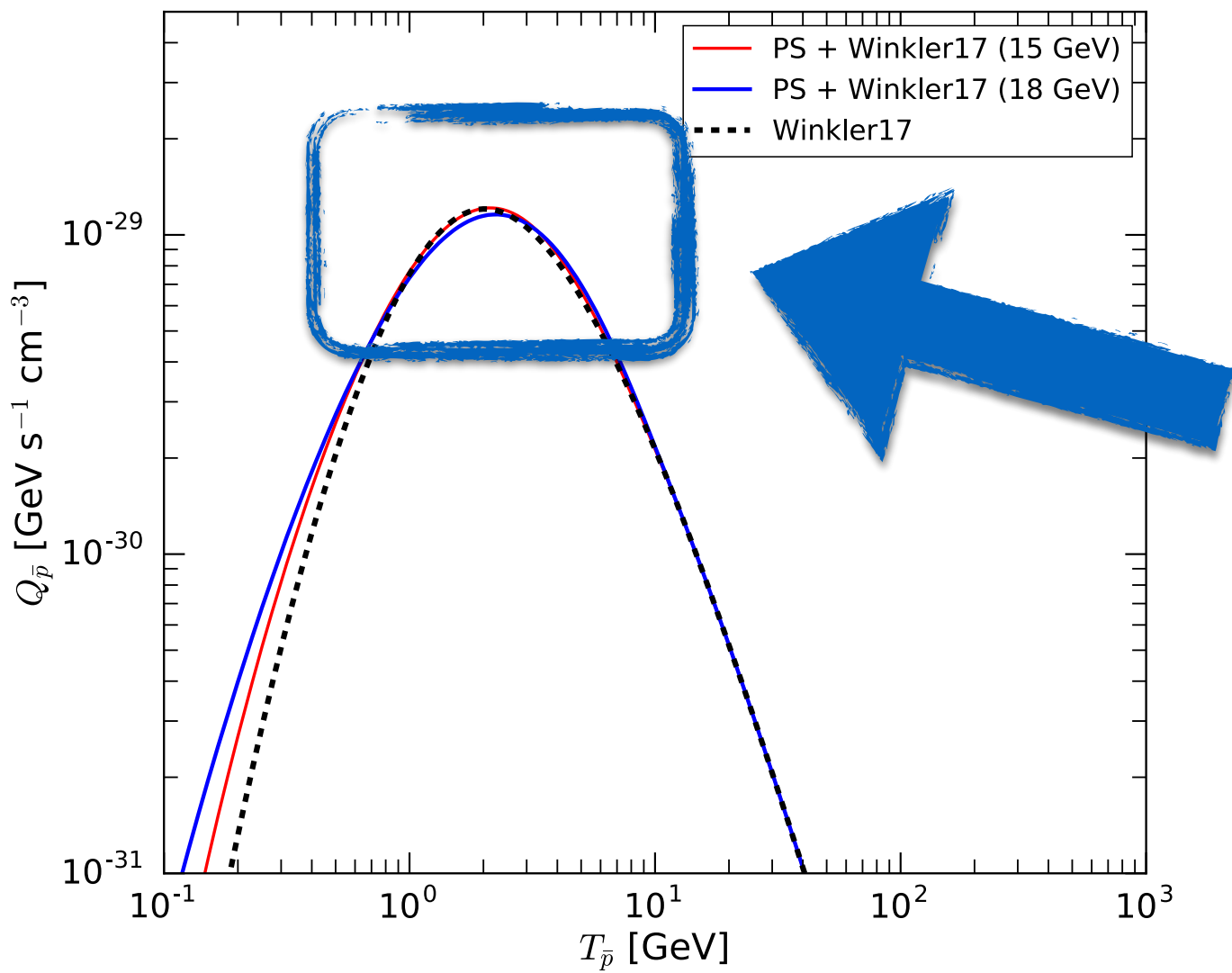
secondary antiproton source term

$$\mathcal{Q}_{\text{sec}}^{\bar{p}}(\vec{x}, \vec{p}) = 4\pi \sum_{j=p,\text{He}} \sum_{k=\text{H,He}} n_k \int dE_j \Phi_j(\vec{p}_j, \vec{x}) \frac{d\sigma}{dp}(j+k \rightarrow i+X)$$



secondary antiproton source term

$$\mathcal{Q}_{\text{sec}}^{\bar{p}}(\vec{x}, \vec{p}) = 4\pi \sum_{j=p,\text{He}} \sum_{k=\text{H,He}} n_k \int dE_j \Phi_j(\vec{p}_j, \vec{x}) \frac{d\sigma}{dp}(j+k \rightarrow i+X)$$

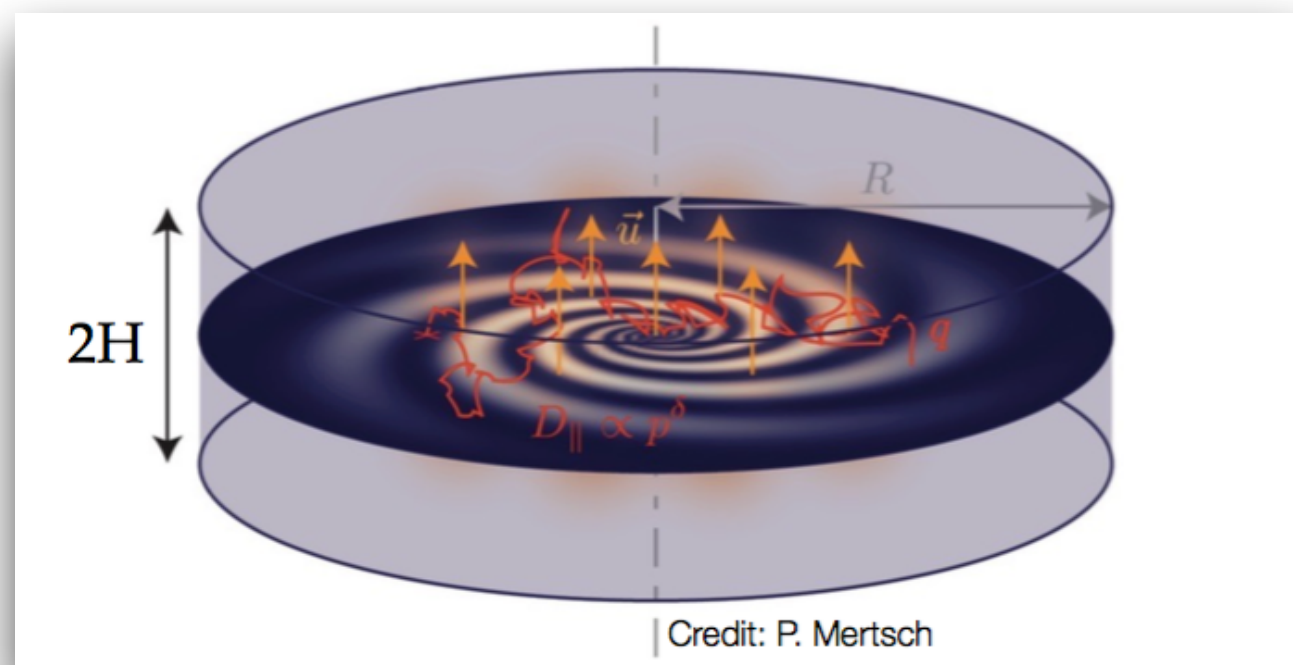


galactic propagation

transport equation

$$\frac{\partial N_i}{\partial t} - \nabla \cdot (D_{xx} \nabla N_i - \vec{v}_w N_i) + \frac{\partial}{\partial p} \left[p^2 D_{pp} \frac{\partial}{\partial p} \left(\frac{N_i}{p^2} \right) \right] - \frac{\partial}{\partial p} \left[\dot{p} N_i - \frac{p}{3} (\vec{\nabla} \cdot \vec{v}_w) N_i \right] = \\ Q - \frac{N_i}{\tau_i^f} + \sum_j \Gamma_{j \rightarrow i}^s(N_j) - \frac{N_i}{\tau_i^r} + \sum_j \frac{N_j}{\tau_{j \rightarrow i}^r}$$

N_i = CR momentum density



The transport model that we consider features **both reacceleration and convection** (with a linearly increasing convection velocity).

We solve the transport equation **numerically**, by using the DRAGON code.

(Evoli et al. JCAP 0810 (2008) 018)

galactic propagation

transport equation

$$\frac{\partial N_i}{\partial t} - \nabla \cdot (\underline{D_{xx}} \nabla N_i - \vec{v}_w N_i) + \frac{\partial}{\partial p} \left[p^2 D_{pp} \frac{\partial}{\partial p} \left(\frac{N_i}{p^2} \right) \right] - \frac{\partial}{\partial p} \left[\dot{p} N_i - \frac{p}{3} (\vec{\nabla} \cdot \vec{v}_w) N_i \right] = Q - \frac{N_i}{\tau_i^f} + \sum_j \Gamma_{j \rightarrow i}^s(N_j) - \frac{N_i}{\tau_i^r} + \sum_j \frac{N_j}{\tau_{j \rightarrow i}^r}$$

N_i = CR momentum density

Motivated by the recent AMS results, we model the spatial diffusion coefficient as a broken power-law in rigidity.

Possible interpretation: transition between diffusion in an **external turbulence** (as the one injected from SNRs) and diffusion onto **CR self-generated waves**

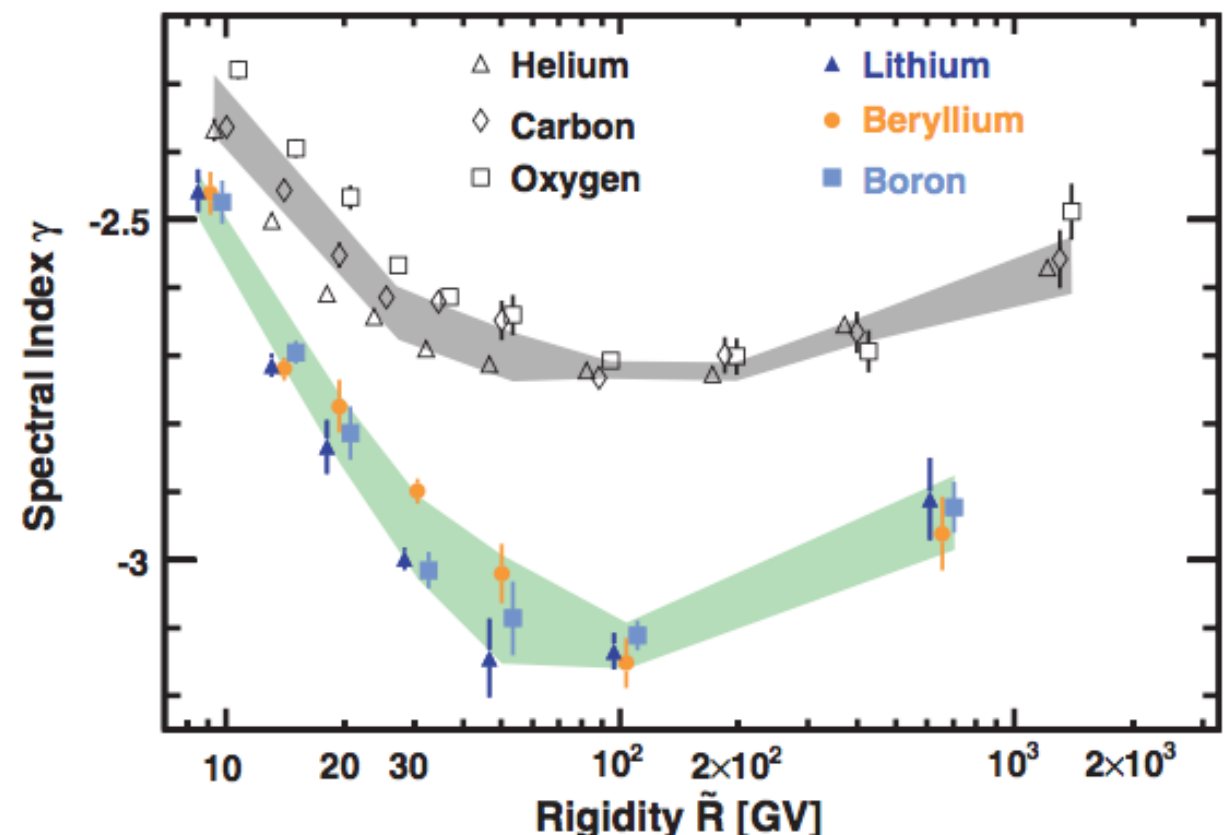


Fig. from Aguilar et al. PRL 120 (2018)

galactic propagation

Fitting a set of **propagation parameters** is a **non-trivial task**.

As it was shown in **G.**

Johannesson et al. ApJ 824 (2016),
the propagation parameters that fit
low-mass isotopes (p, He and pbar) are **significantly different**
than the ones that are found by
fitting the “**usual**” light elements
(Be, B, C, N, O).

How do we deal with this?

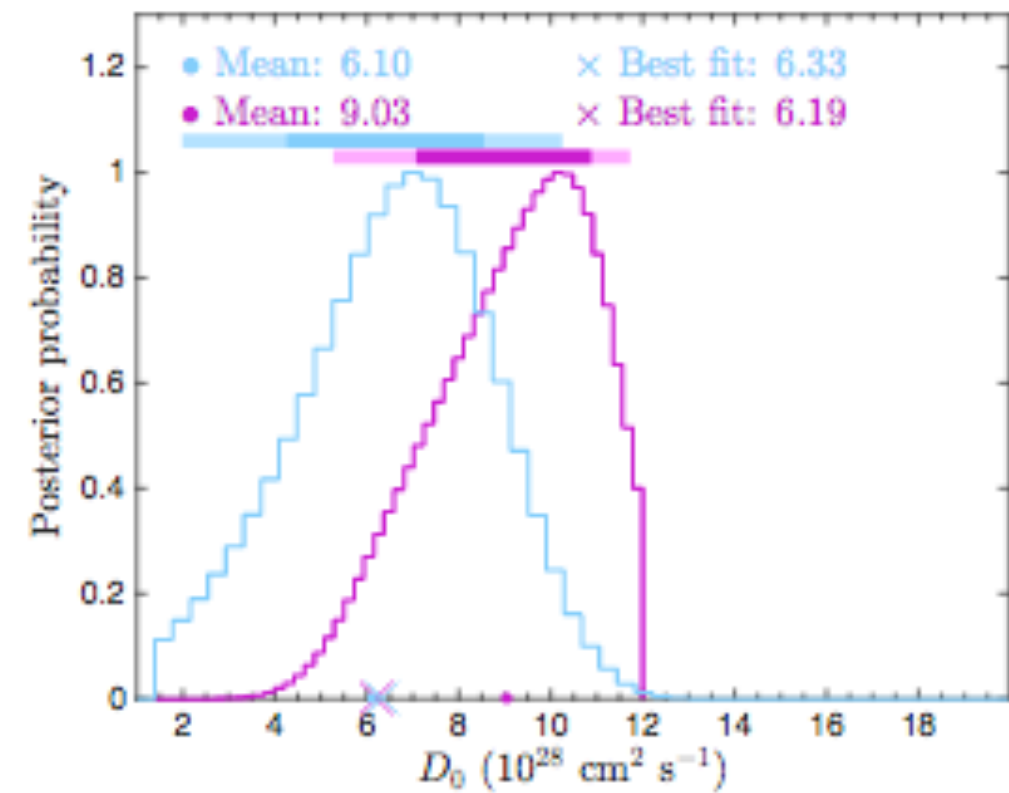
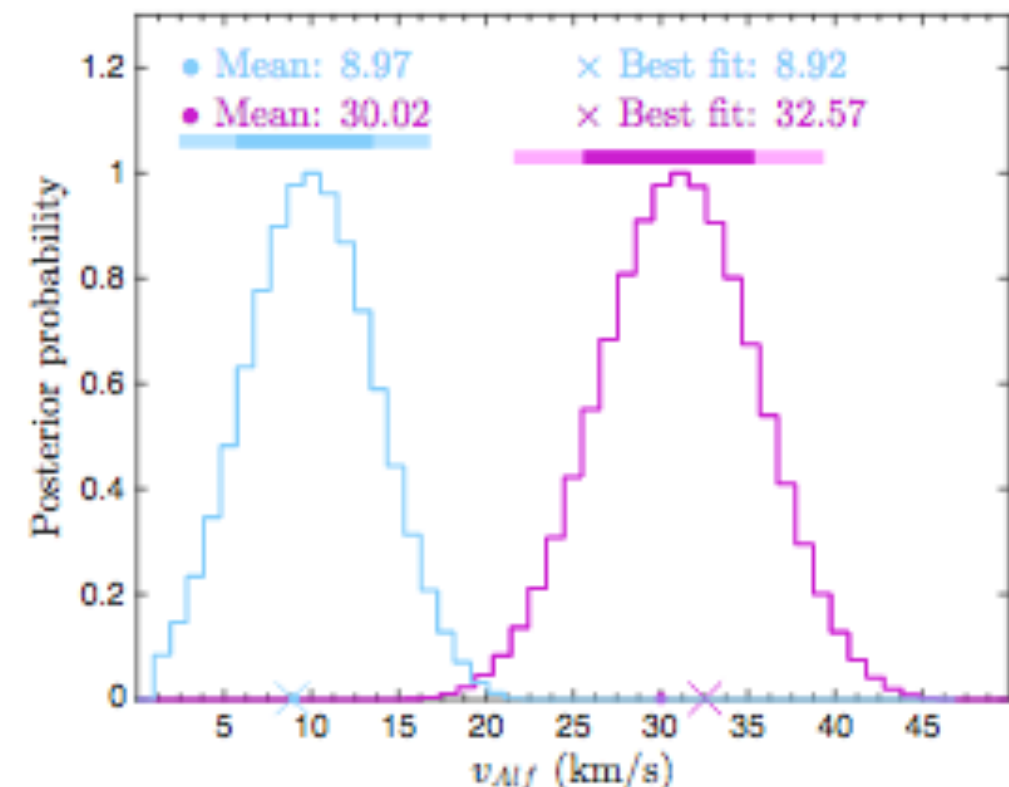


Fig. adapted from **G. Johannesson et al. ApJ 824 (2016)**



galactic propagation

We adopt **two different strategies** to fit the propagation parameters:

- **We fit p, He and \bar{p} data alone**

This means that we assume that **light isotopes** and **heavier nuclei** have **two different propagation histories**.

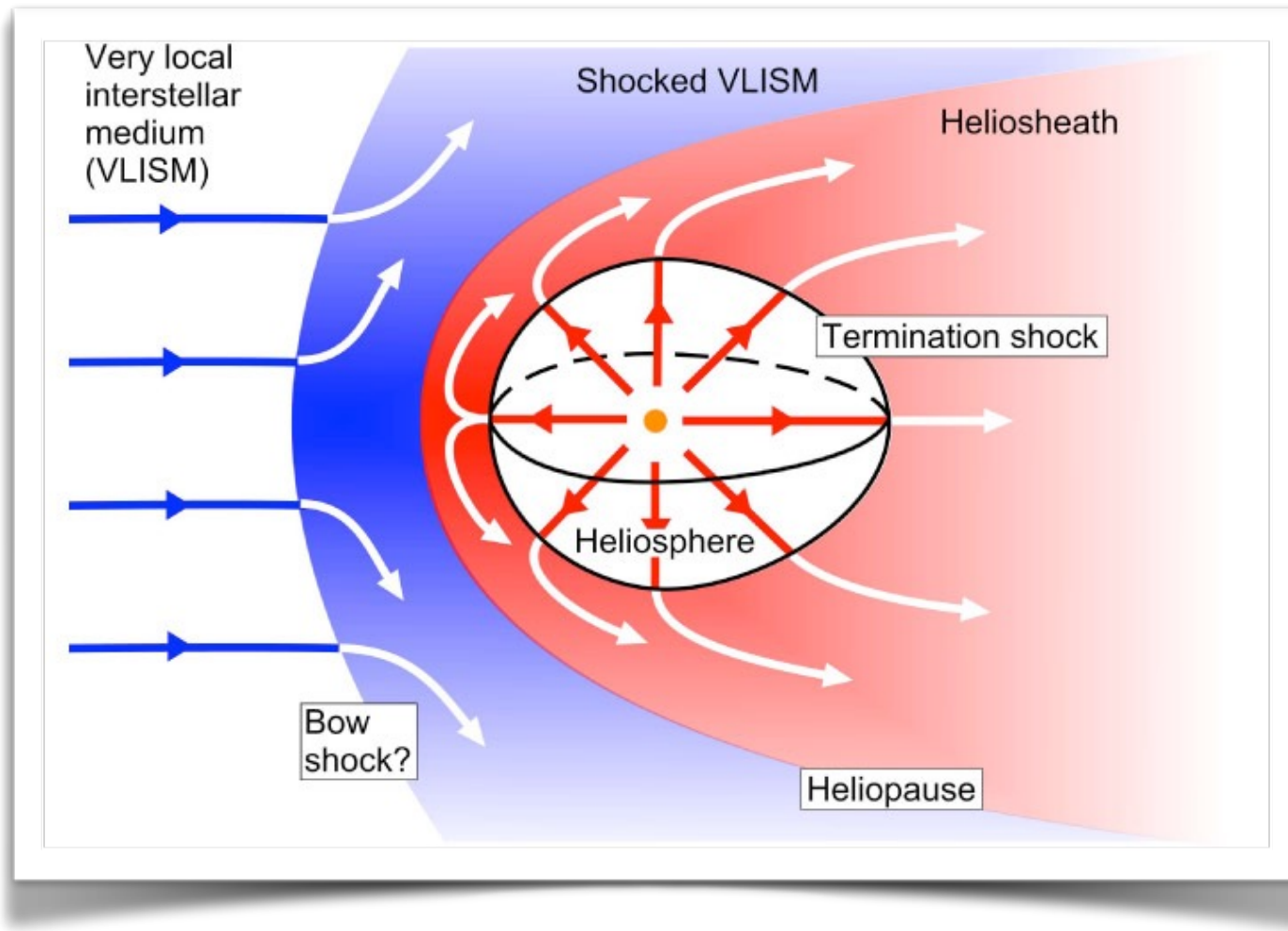
Method 1

- **We fit p, He, B/C and C data. We assign to the \bar{p} flux a free normalisation (the one that provides the best fit).**

This is compatible to assume that the **difference in the propagation parameters** obtained by fitting light isotopes and heavier nuclei is due to **uncertainties in the secondary antiproton production** cross section.

Method 2

solar modulation



force-field approximation:

$$\Phi_{\text{TOA}}(T_{\text{TOA}}) = \frac{T_{\text{TOA}}(T_{\text{TOA}} + 2M)}{T_{\text{LIS}}(T_{\text{LIS}} + 2M)} \Phi_{\text{LIS}}(T_{\text{LIS}})$$

$$\frac{T_{\text{TOA}}}{A} = \frac{T_{\text{LIS}}}{A} - \frac{|Z|}{A} \varphi$$

charge-dependent modulation : we allow for a different value of the Force-field potential for each CR species under consideration

galactic propagation

Method 1

| | Winkler | Winkler + PS 15 GeV | Winkler + PS 18 GeV |
|--|---------|------------------------|------------------------|
| D_0 [$10^{28} \text{ cm}^2 \text{s}^{-1}$] | 3.57 | 3.57 | 3.58 |
| δ_1 | 0.47 | 0.47 | 0.47 |
| δ_2 | 0.37 | 0.38 | 0.38 |
| \mathcal{R}_b [GV] | 179.63 | 179.59 | 179.18 |
| v_A [km s^{-1}] | 23.74 | 23.88 | 23.93 |
| dv_c/dz [$\text{km s}^{-1} \text{kpc}^{-1}$] | 0.70 | 0.70 | 0.74 |
| $\gamma_{p,1}$ | 2.13 | 2.13 | 2.13 |
| $\gamma_{p,2}$ | 2.39 | 2.39 | 2.39 |
| ρ_p [GV] | 10.16 | 10.17 | 10.16 |
| $\gamma_{He,1}$ | 2.18 | 2.17 | 2.17 |
| $\gamma_{He,2}$ | 2.30 | 2.30 | 2.30 |
| ρ_{He} [GV] | 10.10 | 10.09 | 10.09 |
| φ_p [GV] | 0.76 | 0.77 | 0.76 |
| φ_{He} [GV] | 0.61 | 0.60 | 0.59 |
| $\varphi_{\bar{p}}$ [GV] | 0.96 | 0.99 | 1.00 |

| Obs. | Winkler | Winkler + PS (15 GeV) | Winkler + PS (18 GeV) |
|----------------------------|---------|-----------------------|-----------------------|
| p (72 data points) | 60.6 | 61.9 | 60.7 |
| He (68 data points) | 39.4 | 38.1 | 37.7 |
| \bar{p} (57 data points) | 84.3 | 75.8 | 49.2 |
| Total (197 data points) | 184.2 | 175.8 | 147.6 |

Method 2

$$D_0 = 3.99 \times 10^{28} \text{ cm}^2 \text{s}^{-1}$$

$$\delta_1 = 0.43$$

$$\delta_2 = 0.35$$

$$v_A = 27.07 \text{ km s}^{-1}$$

$$dv_c/dz = 0.7 \text{ km s}^{-1} \text{kpc}^{-1}$$

$$\gamma_{p,1} = 2.08$$

$$\gamma_{p,2} = 2.40$$

$$\rho_p = 9.64 \text{ GV}$$

$$\gamma_{He,1} = 2.16$$

$$\gamma_{He,2} = 2.32$$

$$\rho_{He} = 10.18 \text{ GV}$$

$$\gamma_{C,1} = 2.28$$

$$\gamma_{C,2} = 2.37$$

$$\rho_C = 10.30 \text{ GV}$$

| Model | $N_{\bar{p}}$ | $\varphi_{\bar{p}}$ | $\chi^2_{\bar{p}}$ [57 data points] |
|---------------------|---------------|---------------------|-------------------------------------|
| Winkler | 0.96 | 0.73 | 81.04 |
| Winkler + PS 15 GeV | 0.96 | 0.76 | 74.00 |
| Winkler + PS 18 GeV | 0.97 | 0.81 | 49.8 |

galactic propagation

Method 1

| | Winkler | Winkler + PS 15 GeV | Winkler + PS 18 GeV |
|--|---------|------------------------|------------------------|
| D_0 [$10^{28} \text{ cm}^2 \text{s}^{-1}$] | 3.57 | 3.57 | 3.58 |
| δ_1 | 0.47 | 0.47 | 0.47 |
| δ_2 | 0.37 | 0.38 | 0.38 |
| \mathcal{R}_b [GV] | 179.63 | 179.59 | 179.18 |
| v_A [kms $^{-1}$] | 23.74 | 23.88 | 23.93 |
| dv_c/dz [kms $^{-1}$ kpc $^{-1}$] | 0.70 | 0.70 | 0.74 |
| $\gamma_{p,1}$ | 2.13 | 2.13 | 2.13 |
| $\gamma_{p,2}$ | 2.39 | 2.39 | 2.39 |
| ρ_p [GV] | 10.16 | 10.17 | 10.16 |
| $\gamma_{He,1}$ | 2.18 | 2.17 | 2.17 |
| $\gamma_{He,2}$ | 2.30 | 2.30 | 2.30 |
| ρ_{He} [GV] | 10.10 | 10.09 | 10.09 |
| φ_p [GV] | 0.76 | 0.77 | 0.76 |
| φ_{He} [GV] | 0.61 | 0.60 | 0.59 |
| $\varphi_{\bar{p}}$ [GV] | 0.96 | 0.99 | 1.00 |

| Obs. | Winkler | Winkler + PS (15 GeV) | Winkler + PS (18 GeV) |
|----------------------------|---------|-----------------------|-----------------------|
| p (72 data points) | 60.6 | 61.9 | 60.7 |
| \bar{p} (57 data points) | 84.3 | 75.8 | 49.2 |
| Total (129 data points) | 134.2 | 175.8 | 117.8 |

In both cases, using the phase space model at low energies leads to a decrease in the chi-square

Method 2

$$D_0 = 3.99 \times 10^{28} \text{ cm}^2 \text{s}^{-1}$$

$$\delta_2 = 0.35$$

$$dv_c/dz = 0.7 \text{ km s}^{-1} \text{kpc}^{-1}$$

$$\gamma_{p,2} = 2.40$$

$$\gamma_{He,1} = 2.16$$

$$\rho_{He} = 10.18 \text{ GV}$$

$$\gamma_{C,2} = 2.37$$

$$\delta_1 = 0.43$$

$$v_A = 27.07 \text{ km s}^{-1}$$

$$\gamma_{p,1} = 2.08$$

$$\rho_p = 9.64 \text{ GV}$$

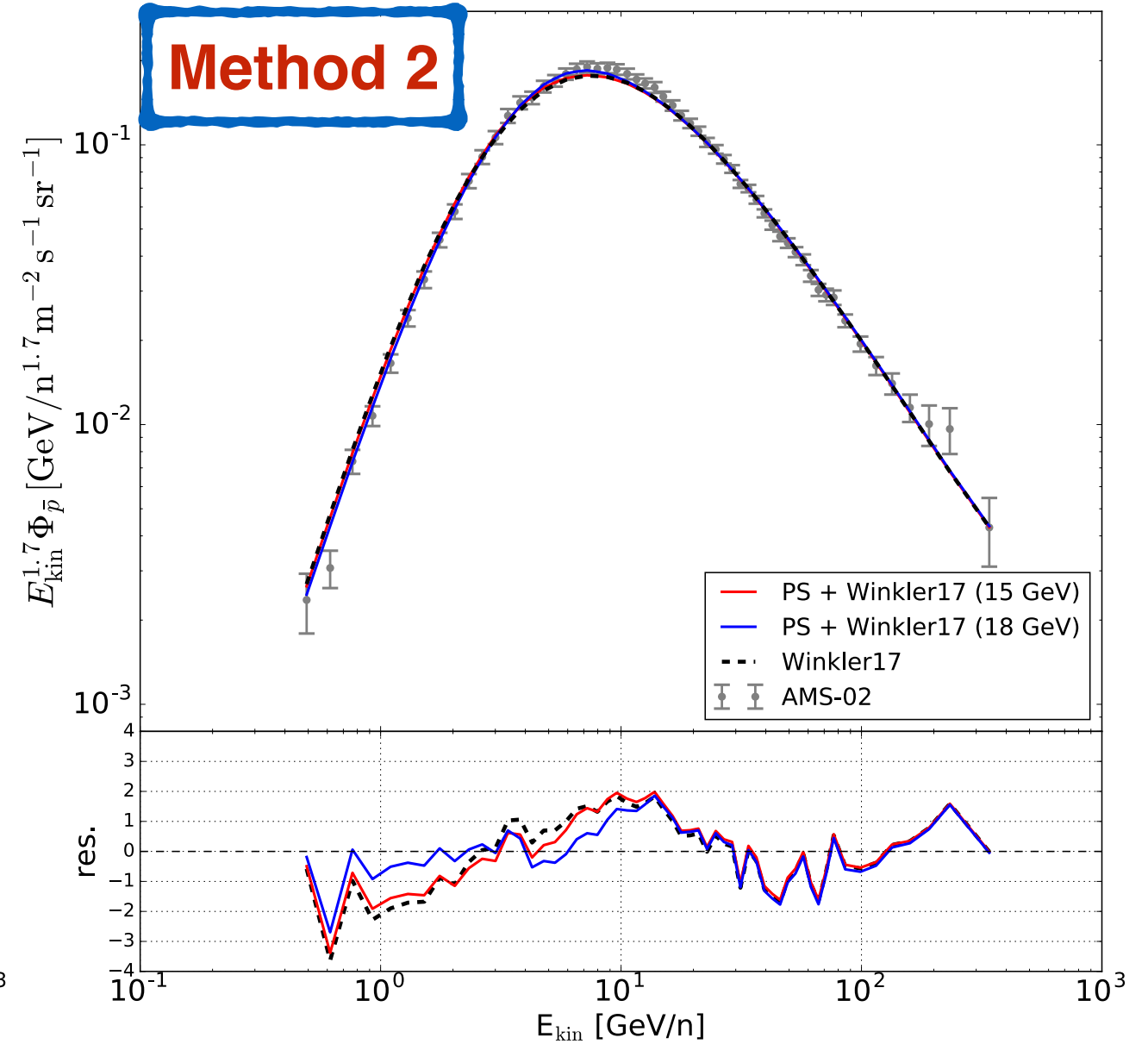
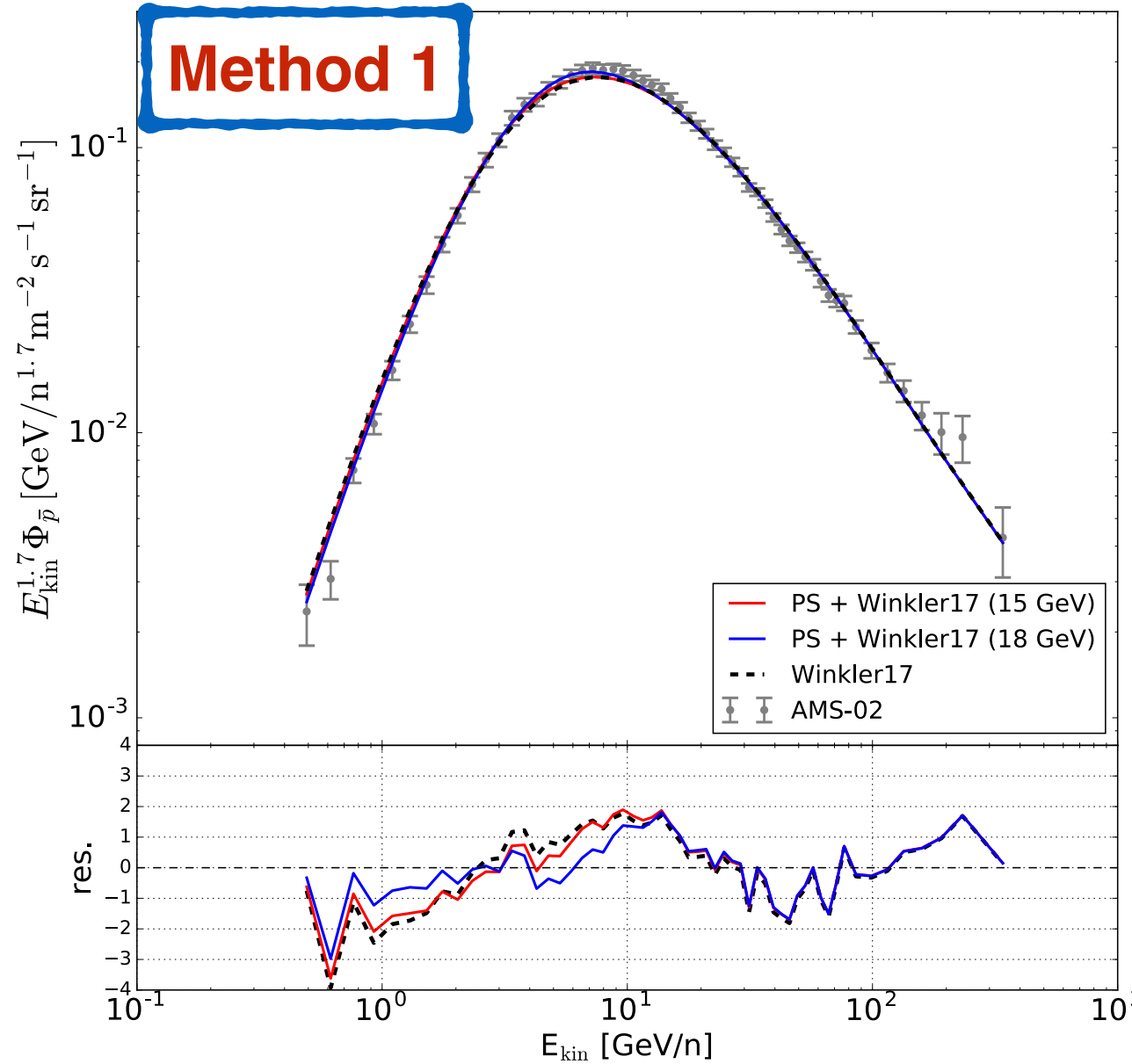
$$\gamma_{He,2} = 2.32$$

$$\gamma_{C,1} = 2.28$$

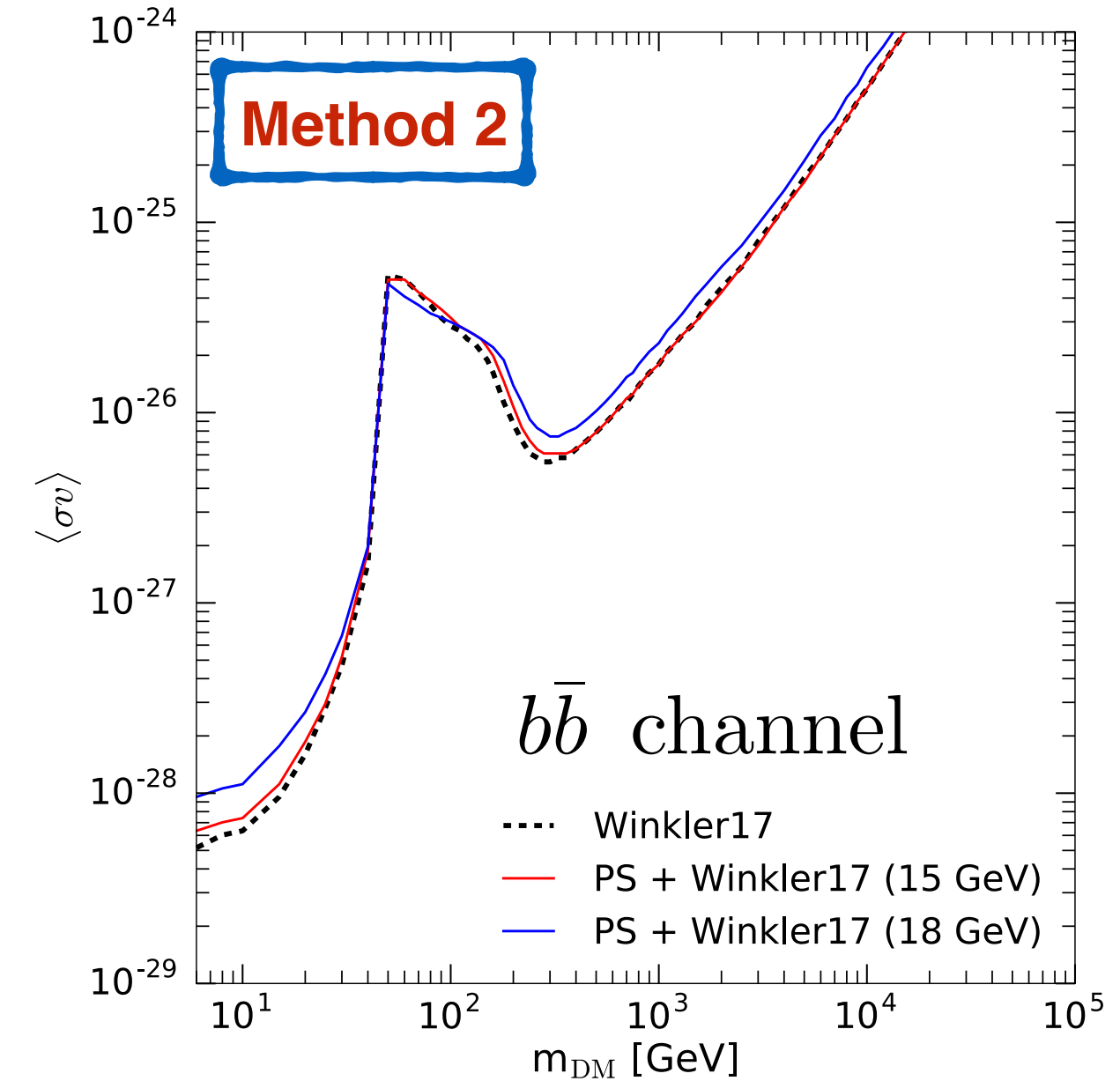
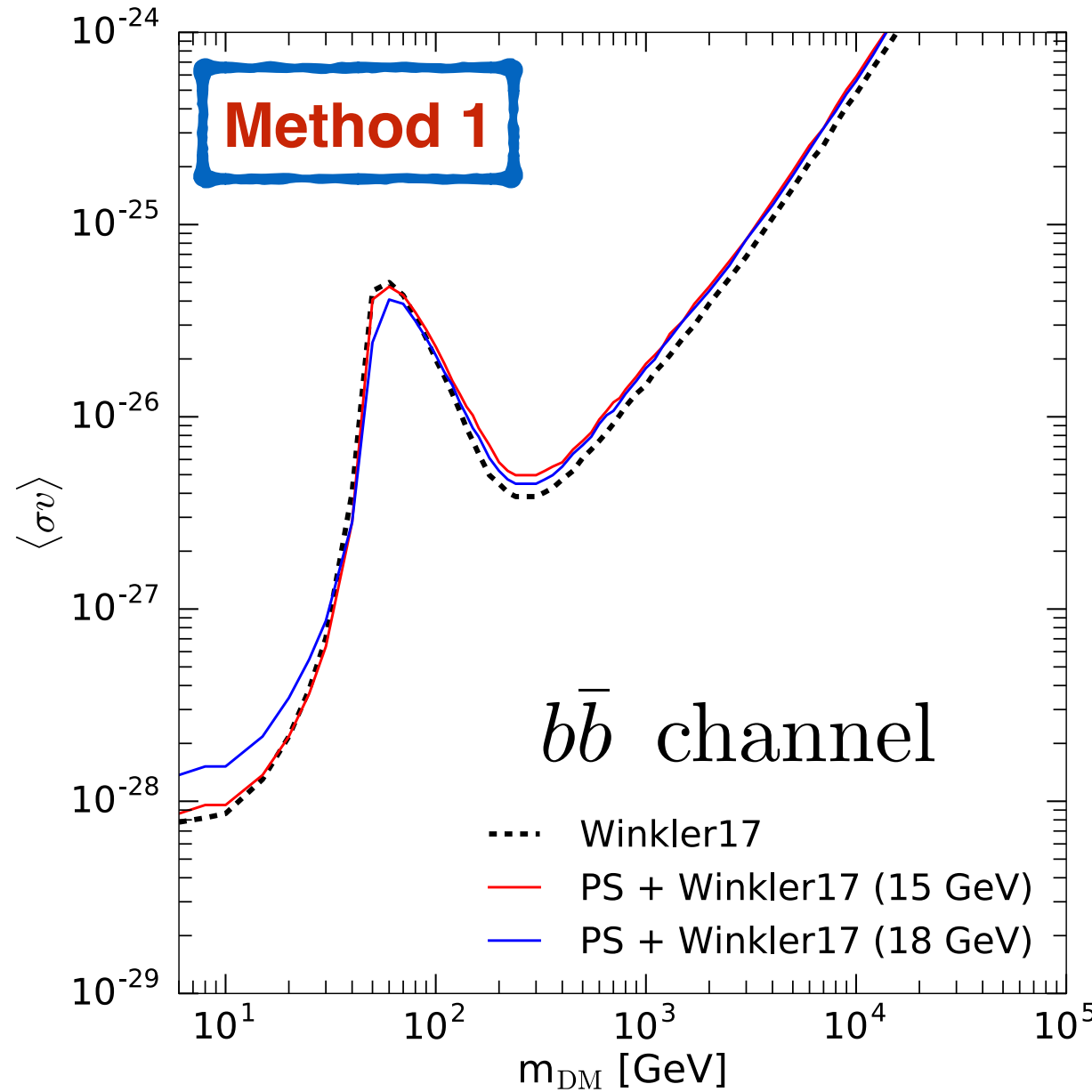
$$\rho_C = 10.30 \text{ GV}$$

| Model | $N_{\bar{p}}$ | $\varphi_{\bar{p}}$ | $\chi^2_{\bar{p}}$ [57 data points] |
|---------------------|---------------|---------------------|-------------------------------------|
| Winkler | 0.96 | 0.73 | 81.04 |
| Winkler + PS 15 GeV | 0.96 | 0.76 | 74.00 |
| Winkler + PS 18 GeV | 0.97 | 0.81 | 49.8 |

results - secondary antiproton fluxes

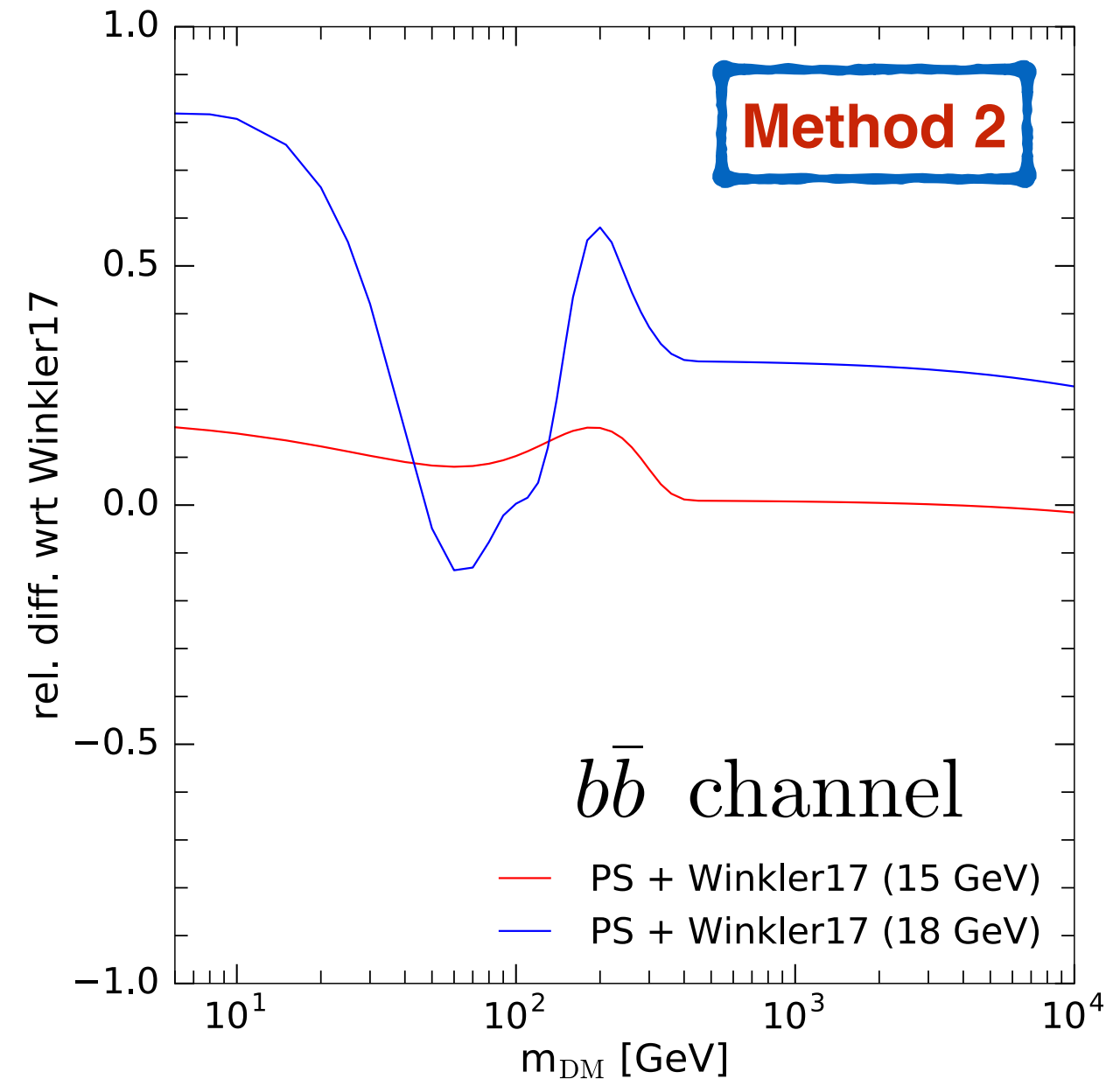
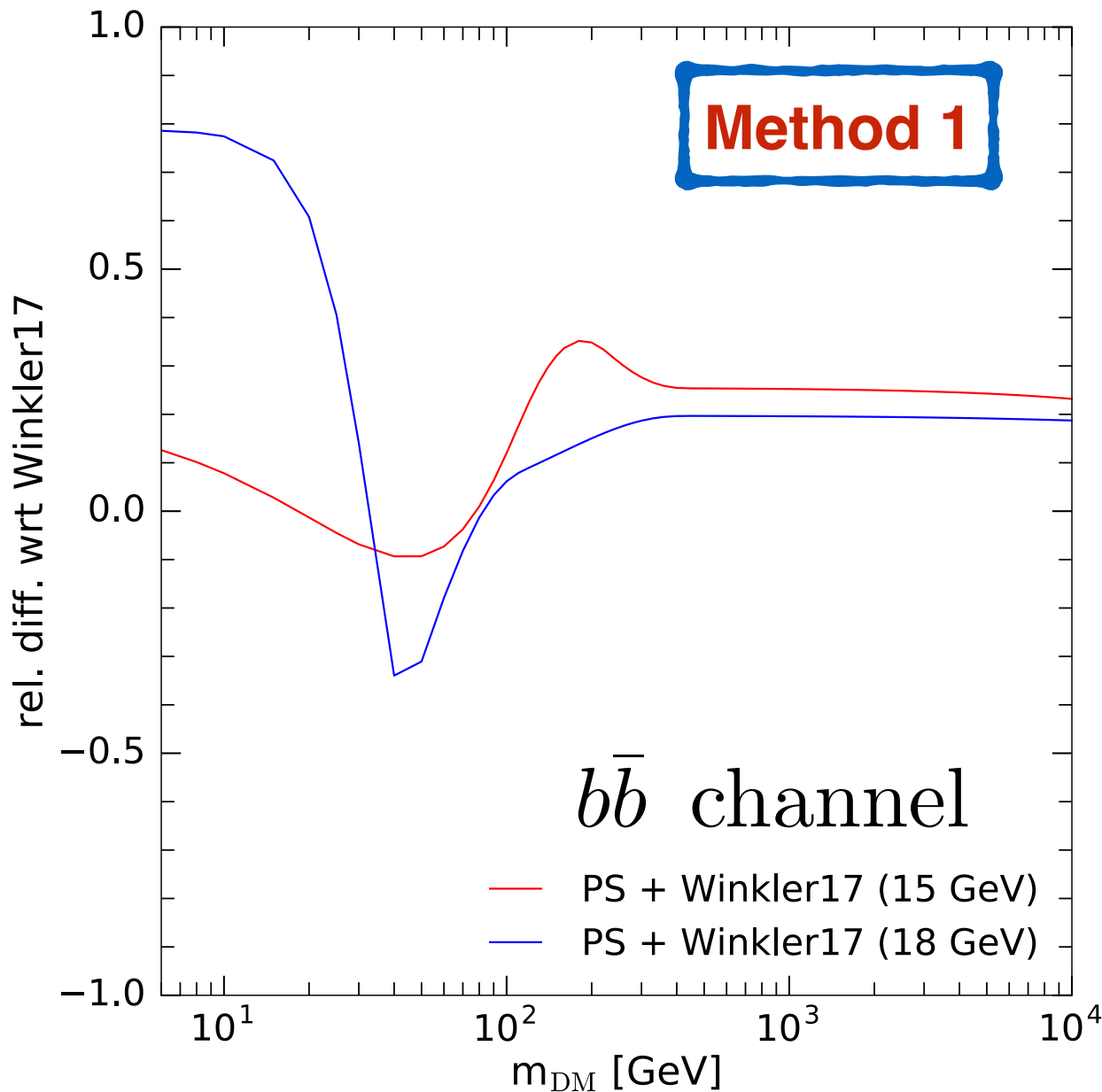


results - dark matter bound



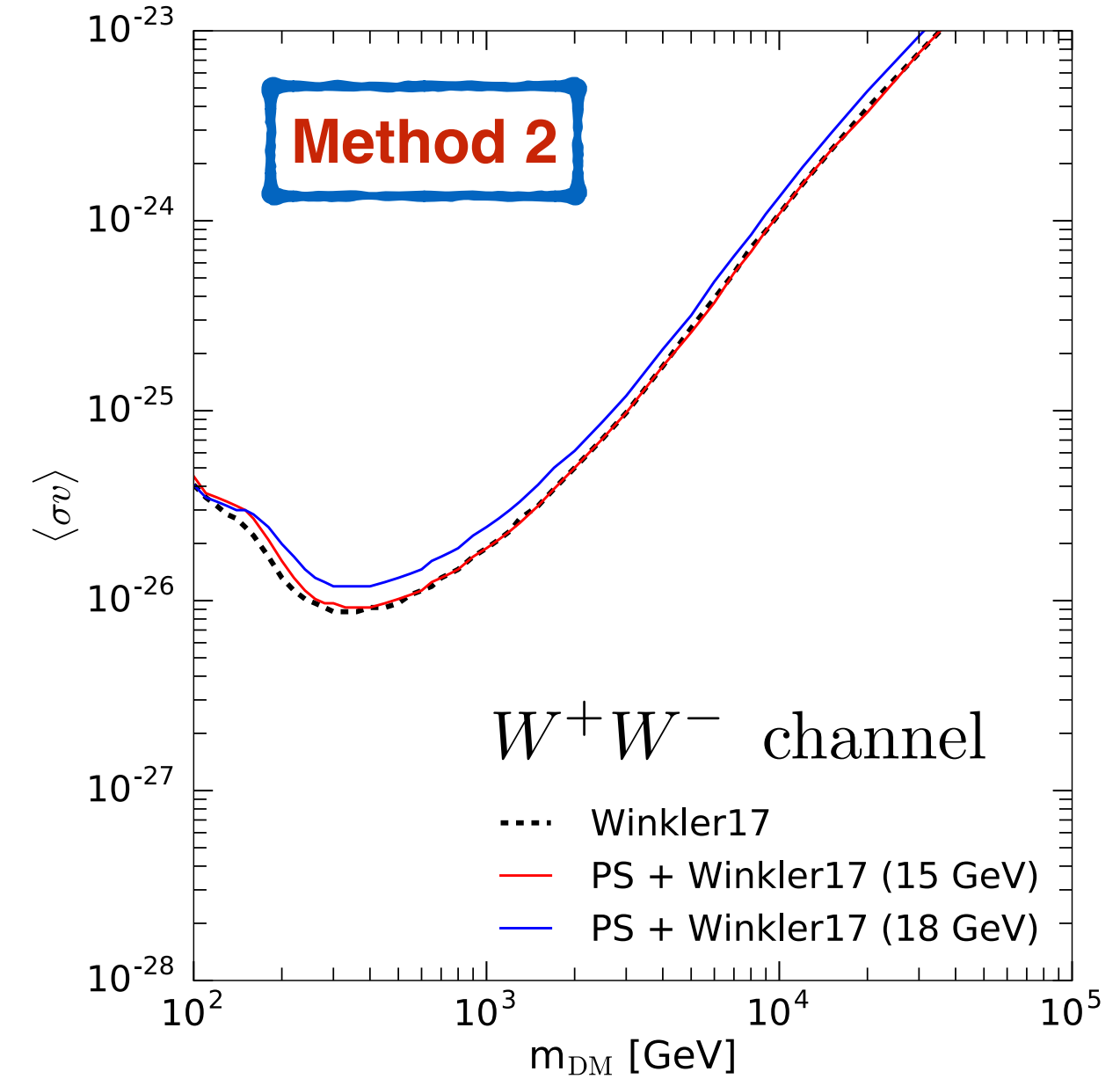
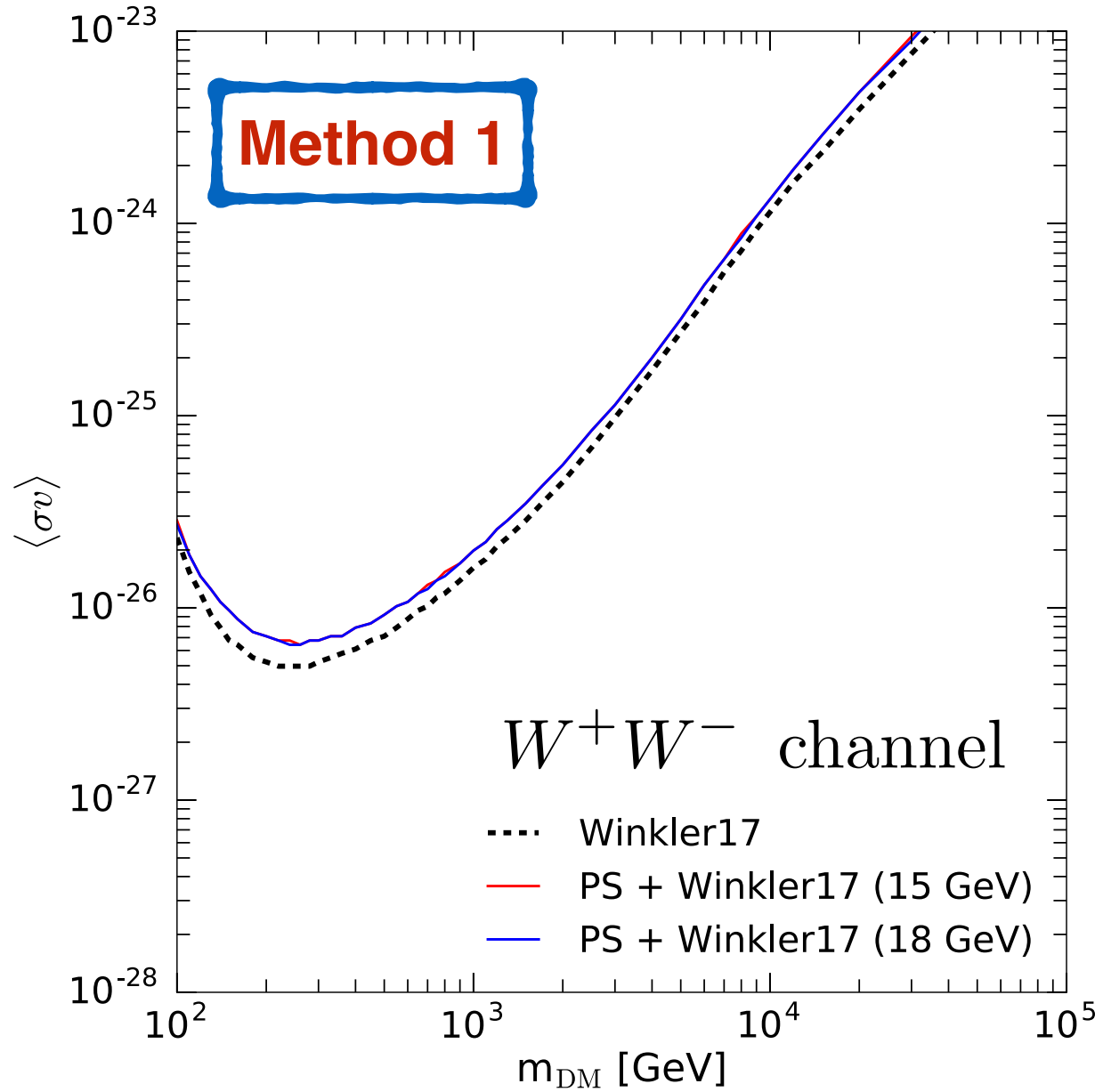
- For **Method 1**, we marginalise over the **force-field potential**
- For **Method 2**, we marginalise over the **force-field potential** and the **normalisation of the secondary antiproton flux**
- Dark matter **spectra** at injection from **PPPC 4 DM ID** ([Cirelli et al. JCAP 1103 \(2011\) 051](#))

results - dark matter bound



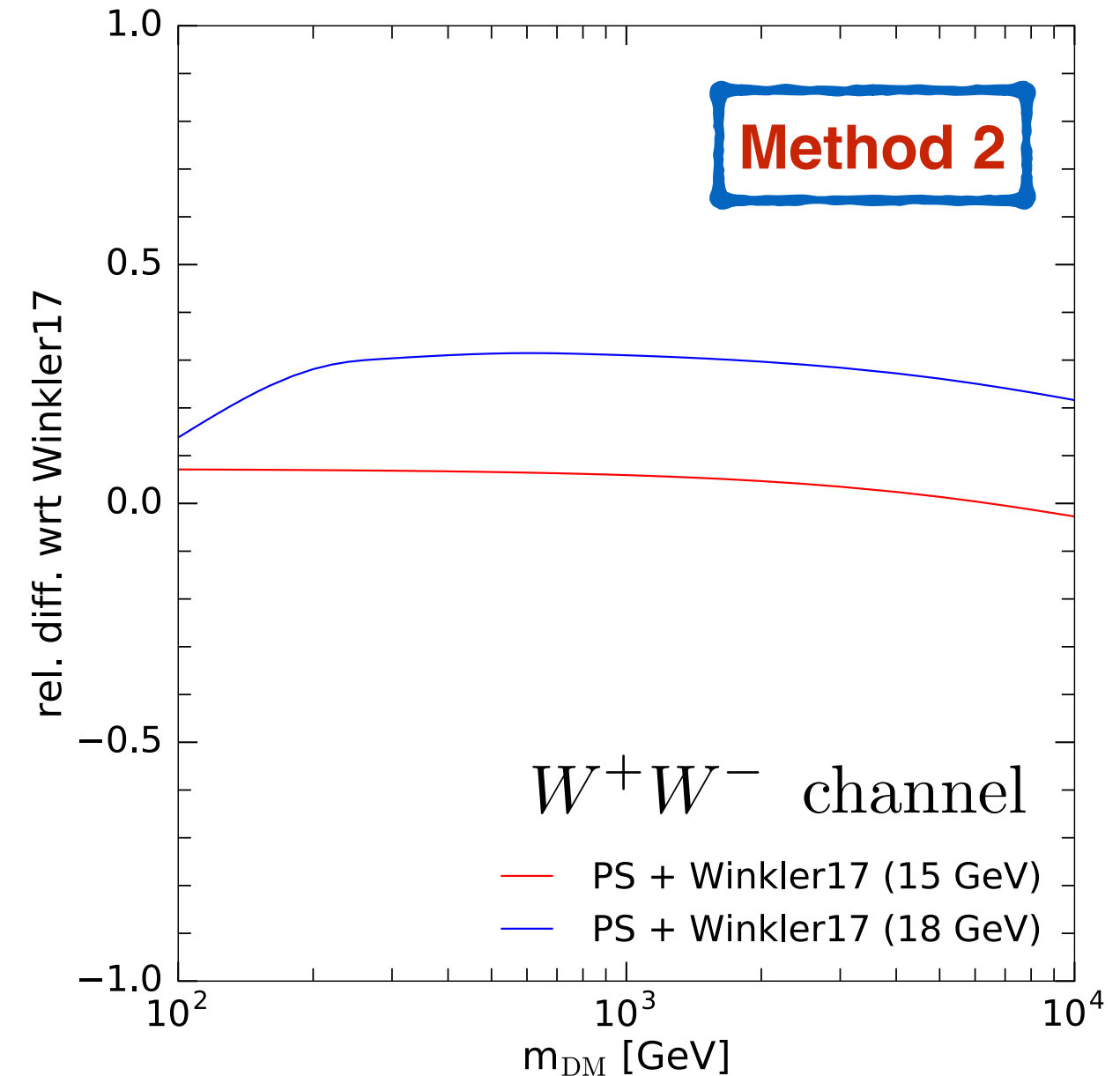
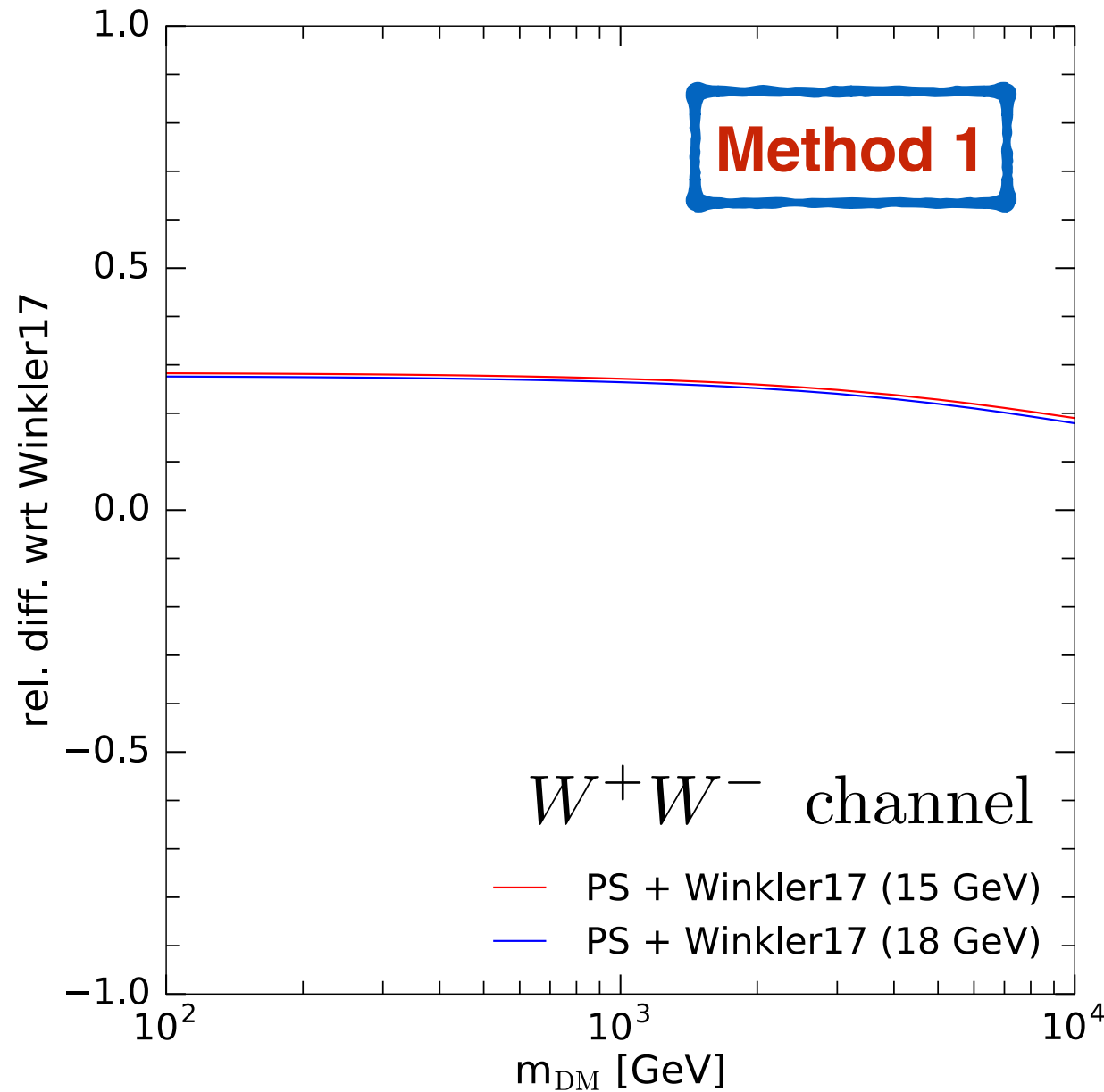
The **difference** with respect to the bounds obtained with the Winkler model can reach **up to 80%**, if the phase space model is used up to high energies, otherwise it **stays within 30%**

results - dark matter bound



- For **Method 1**, we marginalise over the **force-field potential**
- For **Method 2**, we marginalise over the **force-field potential** and the **normalisation of the secondary antiproton flux**
- Dark matter **spectra** at injection from **PPPC 4 DM ID** ([Cirelli et al. JCAP 1103 \(2011\) 051](#))

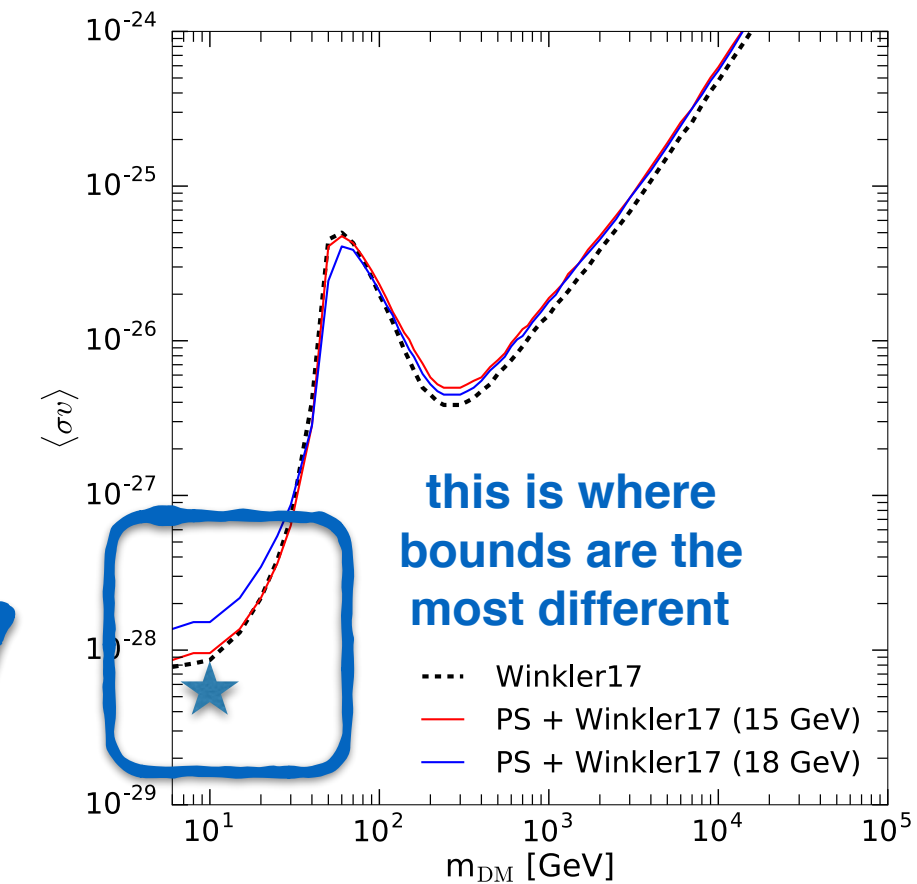
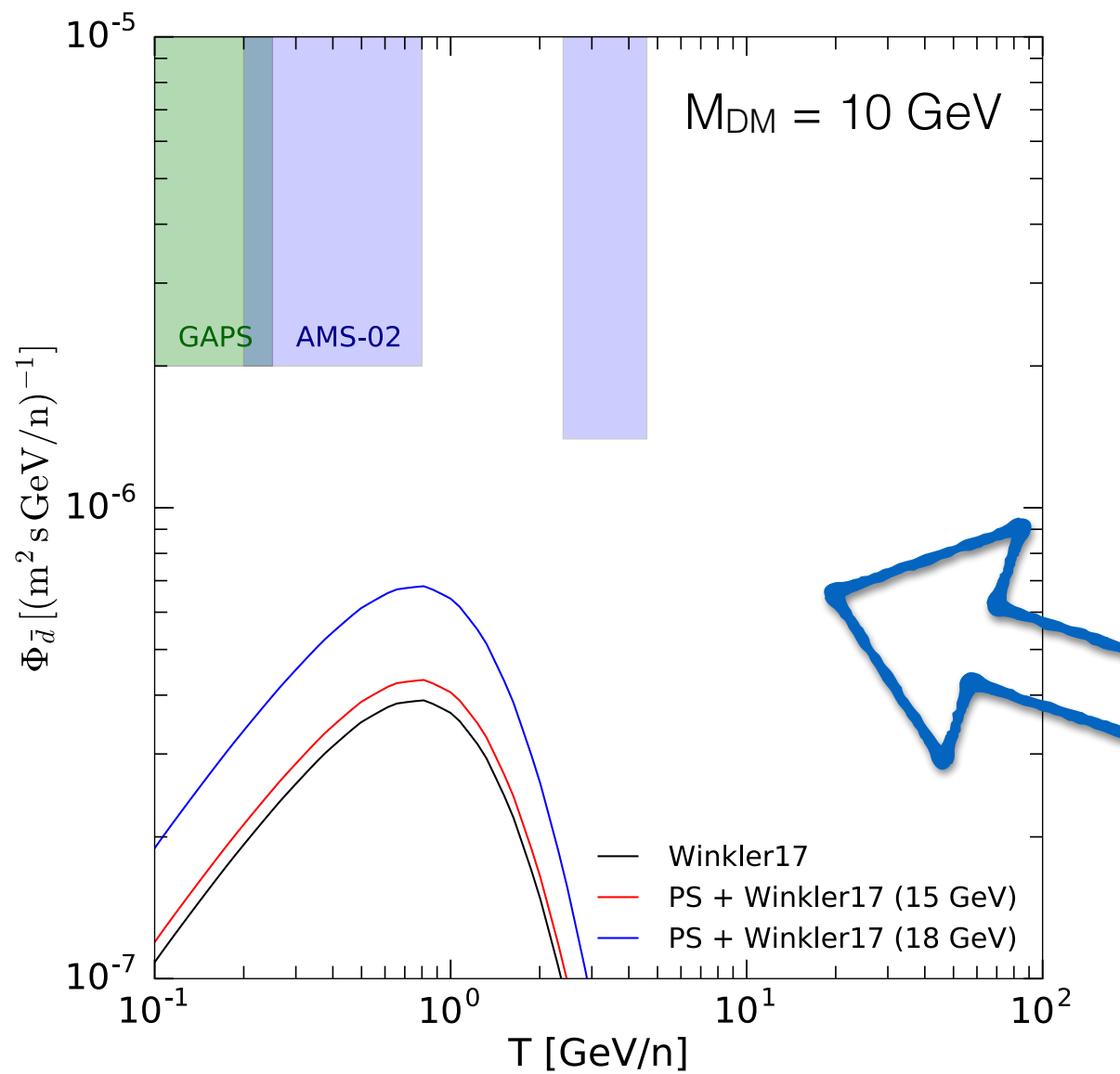
results - dark matter bound



The **difference** with respect to the bounds obtained with the Winkler is **always below 30%**

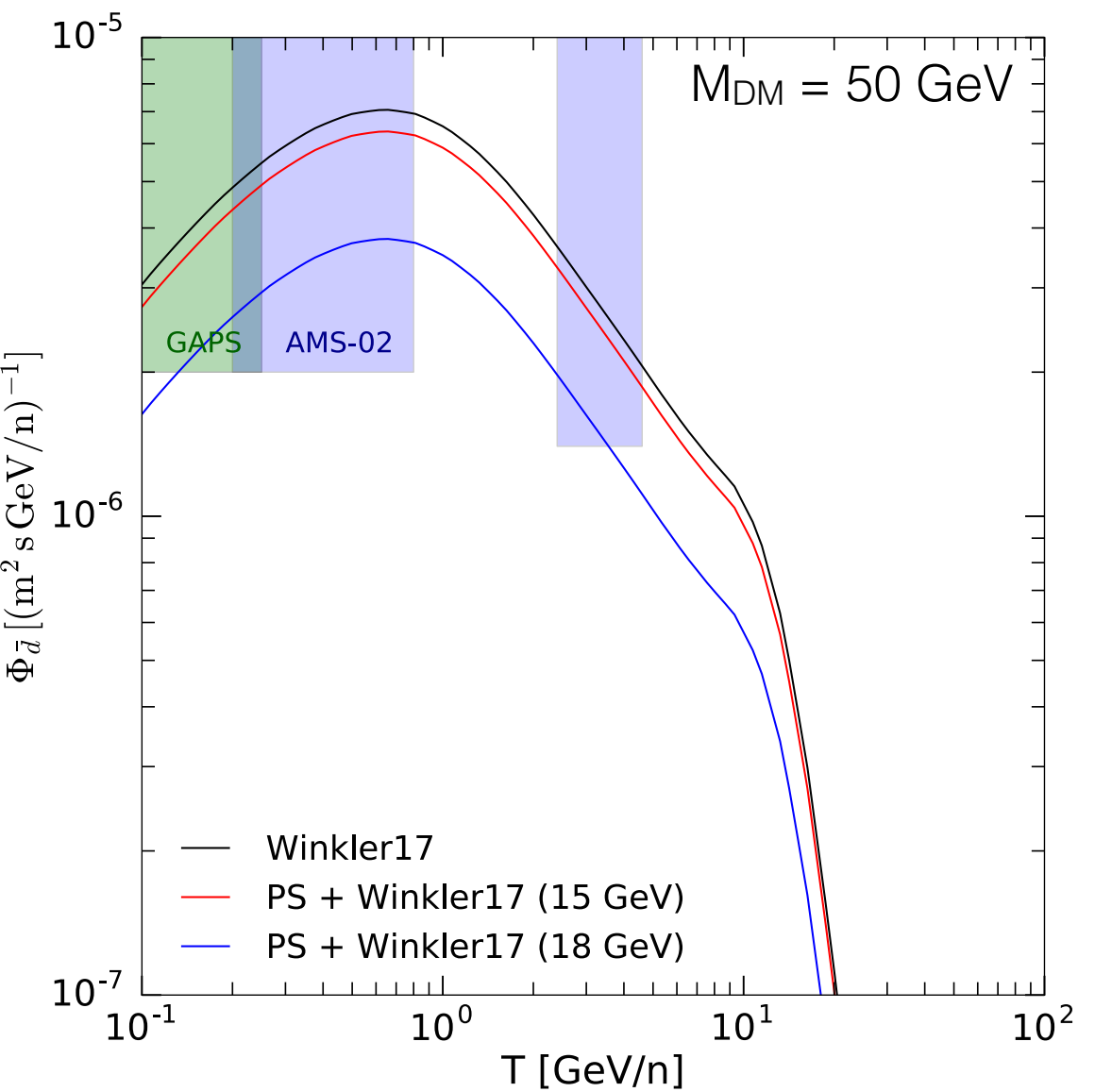
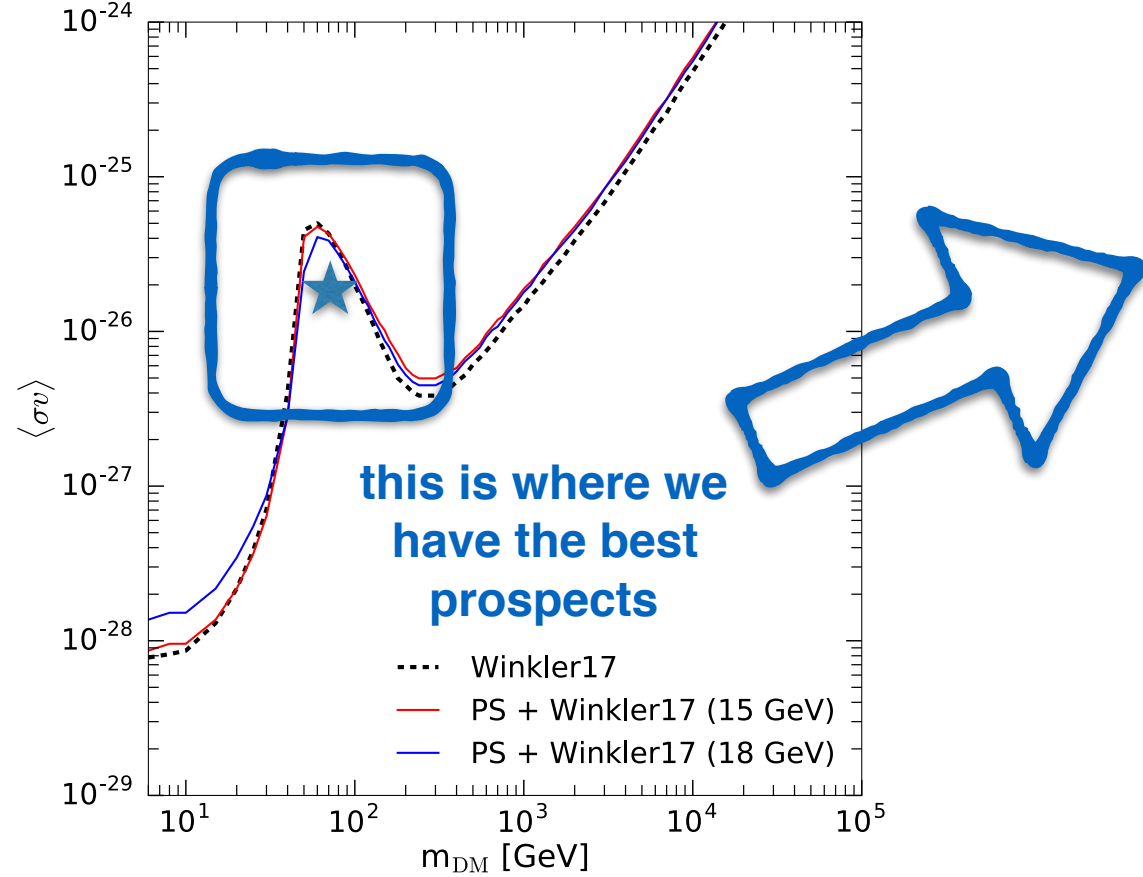
results - antideuteron prospects

Is this difference in the bounds **significative** for what concerns the prospects of **dark matter detection in the antideuteron channel?**



results - antideuteron prospects

Is this difference in the bounds **significative** for what concerns the prospects of **dark matter detection in the antideuteron channel?**



Antideuteron fluxes at injection from **PPPC 4 DM ID** ([Cirelli et al. JCAP 1103 \(2011\) 051](#))

conclusions

We have illustrated a **very simple analytical model** to describe the **low-energy behaviour** of the **secondary antiproton production cross section**

By applying such model we have shown that:

- ▶ The excess in the antiproton flux at around 10 GV **does not appear to be affected** by the modelling of the low-energy cross section
- ▶ The **impact on the dark matter antiproton bounds** can **reach the 20/30%** level (70/80% for the most aggressive configurations)
- ▶ This impact on the antiproton bounds obviously **reflects on the expected antideuteron fluxes**

Obviously, our **phase space model** is very likely to be an **oversimplification**. We are currently working on refining it by including effects that could be relevant (resonances, formation of bound states, final state interactions ...)

back-up slides

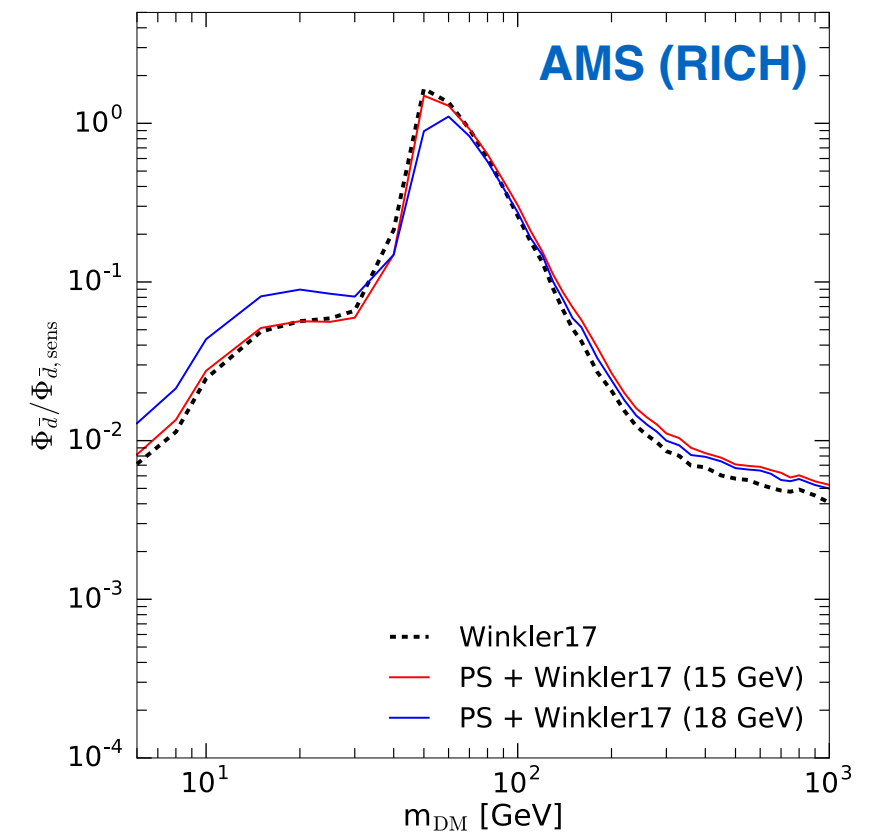
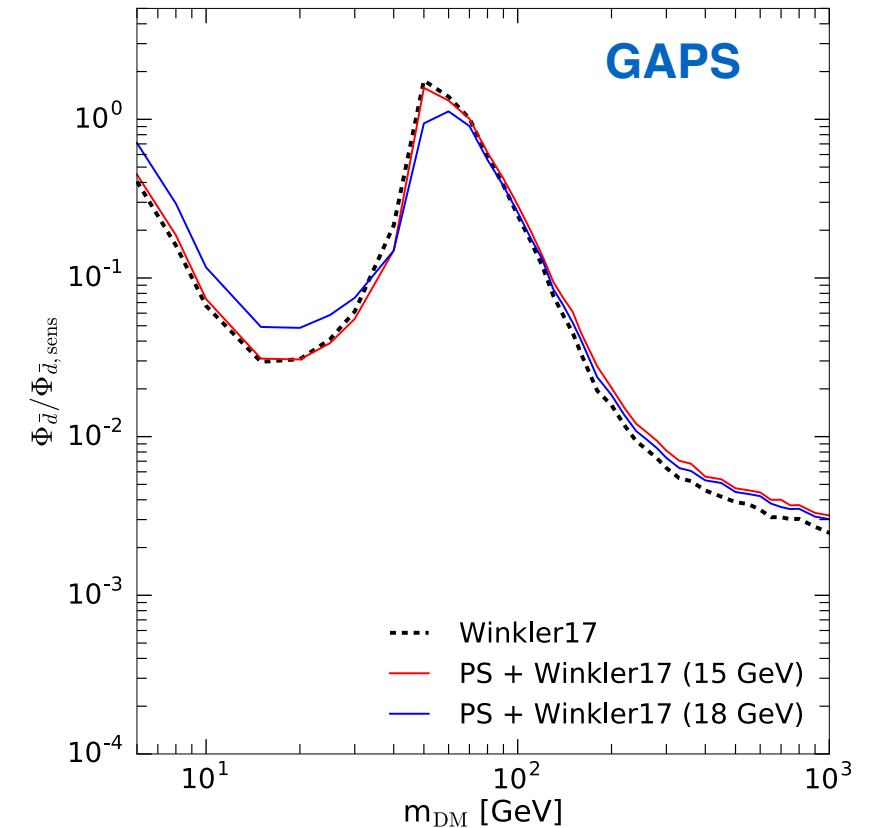
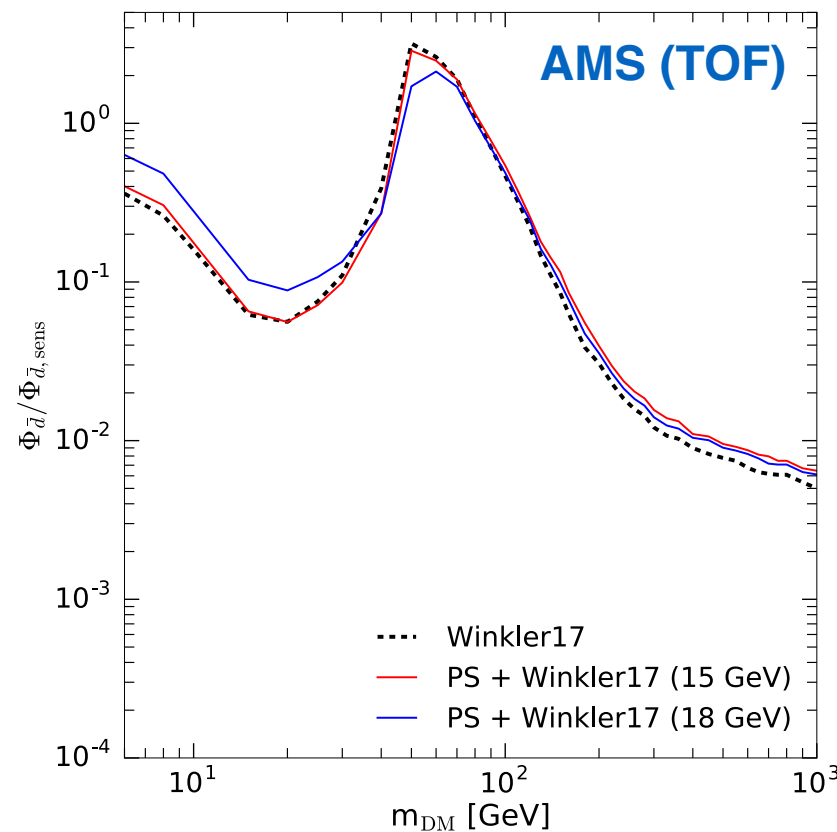
results - antideuteron prospects

We plot

$$\frac{\int_{T_{\text{MIN}}}^{T_{\text{MAX}}} \Phi_{\bar{d}}(T) dT}{\int_{T_{\text{MIN}}}^{T_{\text{MAX}}} \Phi_{\bar{d},\text{sens}}(T) dT}$$

| Detector | $\Phi_{\bar{d},\text{sens}}$ [(m ² s GeV/n) ⁻¹] | T_{min} [GeV/n] | T_{max} [GeV/n] |
|------------------|---|-----------------------------|-----------------------------|
| GAPS [28] | 2×10^{-6} | 0.05 | 0.25 |
| AMS-02 TOF [27] | 2×10^{-6} | 0.2 | 0.8 |
| AMS-02 RICH [27] | 1.4×10^{-6} | 2.4 | 4.6 |

Herms, Ibarra, Vittino, Wild, JCAP 1702 (2017) 018



low energies - the phase space model

Under the simplifying assumption that the amplitude is constant, the n-body phase space term can be **easily derived in a fully analytical way**

The general idea is to introduce intermediate four-momenta $q_a = \sum_{i \in a} p_i$ by inserting unities in the form:

$$1 = \int \frac{d^4 q_a}{(2\pi)^4} (2\pi)^4 \delta(q_a - \sum_{i \in a} p_i) \theta(q_a^0)$$

Furthermore, we can relate q_a to a mass-square-like quantity s_a by using

$$1 = \int \frac{ds_a}{2\pi} 2\pi \delta(s_a - q_a^2) = \int \frac{ds_a}{2\pi} 2\pi \frac{\delta(q_a^0 - E_a)}{2E_a} \theta(q_a^0)$$

low energies - the phase space model

Under the simplifying assumption that the amplitude is constant, the n-body phase space term can be **easily derived in a fully analytical way**

By putting together the above equations we get:

$$1 = \int \frac{ds_a}{2\pi} \int \frac{d^3 q_a}{(2\pi)^3} \frac{1}{2E_a} (2\pi)^4 \delta(q_a - \sum_{i \in a} p_i)$$

Which, if plugged into the phase space term, gives:

$$\begin{aligned} \int d\Phi_n(P; p_1, \dots, p_n) &= \int \frac{ds_a}{2\pi} \frac{d^3 q_a}{(2\pi)^3} \frac{1}{2E_a} \int \frac{d^3 p_n}{(2\pi)^3} \frac{1}{2E_n} (2\pi)^4 \delta(P - q_a - q_n) \times \\ &\quad \times \prod_{i=1}^{n-1} \int \frac{d^3 p_i}{(2\pi)^3} \frac{1}{2E_i} (2\pi)^4 \delta(q_a - \sum_{j=1}^{n-1} p_j) \end{aligned}$$

where we have a **2-body phase space** and a **(n-1)-body phase space** terms